AD-A042 440 OHIO STATE UNIV COLUMBUS ELECTROSCIENCE LAB F/G 9/5
ADAPTIVE ARRAY PERFORMANCE WITH CODED FM SIGNALS.(U)
MAY 77 I K LAO, R T COMPTON N00019-77-C-0156
UNCLASSIFIED ESL-4618-2 NL

| OF |
AD
A042440

END

DATE
FILMED
8-77

12

ADAPTIVE ARRAY PERFORMANCE WITH CODED FM SIGNALS

I.K. Lao and R.T. Compton, Jr.

The Ohio State University

ElectroScience Laboratory

Department of Electrical Engineering
Columbus, Ohio 43212

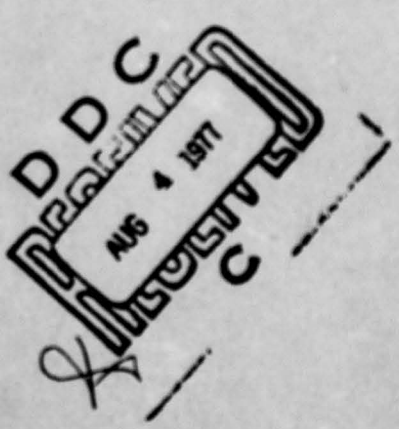

Technical Report 4618-2

May 1977

Contract N00019-77-C-0156

Department of the Navy
Naval Air Systems Command
Washington, D.C. 20361

NOTICES

When Government drawings, specifications, or other data are used for any purpose other than in connection with a definitely related Government procurement operation, the United States Government thereby incurs no responsibility nor any obligation whatsoever, and the fact that the Government may have formulated, furnished, or in any way supplied the said drawings, specifications, or other data, is not to be regarded by implication or otherwise as in any manner licensing the holder or any other person or corporation, or conveying any rights or permission to manufacture, use, or sell any patented invention that may in any way be related thereto.

UNCLASSIFIED

SECURITY CLASSIFICATION OF THIS PAGE (When Data Entered)

REPORT DOCUMENTATION PAGE

READ INSTRUCTIONS BEFORE COMPLETING FORM

1 REPORT NUMBER

2 GOVT ACCESSION NO

3 RECIPIENT'S CATALOG NUMBER

4 TITLE (and Subtitle)

ADAPTIVE ARRAY PERFORMANCE WITH CODED FM SIGNALS.

5 TYPE OF REPORT & PERIOD COVERED

Technical Report

6 PERFORMING ORG. REPORT NUMBER

ESL-4618-2

7 AUTHOR(s)

I.K. Lao and R.T. Compton, Jr.

8 CONTRACT OR GRANT NUMBER(s)

Contract N00019-77-C-0156

9 PERFORMING ORGANIZATION NAME AND ADDRESS

The Ohio State University ElectroScience Laboratory, Department of Electrical Engineering, Columbus, Ohio 43212

10 PROGRAM ELEMENT, PROJECT, TASK AREA & WORK UNIT NUMBERS

Project #N00019-77-PR-RJ004

11 CONTROLLING OFFICE NAME AND ADDRESS

Department of the Navy
Naval Air Systems Command
Washington, D.C. 20361

12 REPORT DATE

May 1977

13 NUMBER OF PAGES

67

14 MONITORING AGENCY NAME & ADDRESS (if different from Controlling Office)

15 SECURITY CLASS. (of this report)

Unclassified

15a DECLASSIFICATION/DOWNGRADING SCHEDULE

16 DISTRIBUTION STATEMENT (of this Report)

APPROVED FOR PUBLIC RELEASE: DISTRIBUTION UNLIMITED

17 DISTRIBUTION STATEMENT (of the abstract entered in Block 20, if different from Report)

18 SUPPLEMENTARY NOTES

The material contained in this report is also used as a Thesis submitted to the Department of Electrical Engineering, The Ohio State University as partial fulfillment for the degree Master of Science.

19 KEY WORDS (Continue on reverse side if necessary and identify by block number)

Adaptive arrays
Frequency modulation
Interference rejection

20 ABSTRACT (Continue on reverse side if necessary and identify by block number)

This report discusses the use of FM signals with adaptive arrays. The FM signals contain an extra pseudonoise bi-phase modulation to enable the adaptive array to distinguish the desired signal from interference. The performance of the array is studied as a function of reference signal modulation delay, code timing delay, and frequency offsets.

DD FORM 1 JAN 73 1473 EDITION OF 1 NOV 65 IS OBSOLETE

UNCLASSIFIED

SECURITY CLASSIFICATION OF THIS PAGE (When Data Entered)

402 251

TABLE OF CONTENTS

CHAPTER I

INTRODUCTION

The objective of this research is to develop an antenna system capable of receiving a FM communication signal in the presence of a strong interference signal without the need for detailed information about signal modulation or the angle of arrival. The basic properties of an adaptive array have been investigated previously[1,2,3] and are well established. In this research we develop an approach for integrating an adaptive array into an FM communication system.

An adaptive array is an array of antenna elements followed by a real time adaptive processor. The antenna array can automatically place pattern nulls in directions from which undesired signals (interference, jamming or clutter) arrive and can also provide gain on a desired signal. Widrow, et al[1], proposed the basic adaptive array feedback algorithm, the so-called LMS algorithm. Applebaum [3] also developed an adaptive array control loop which maximizes the array output signal-to-noise ratio.

In this report we consider an adaptive array based on the LMS algorithm[1]. The general structure of such an array (for two elements) is shown in Figure 1. The incoming signal from each element, $y_i(t)$, is split into in-phase and quadrature components $x_i(t)$. Each component is multiplied by a weight w_i and then summed to produce the array output,

$$S(t) = \sum_{i=1}^{4} w_i x_i(t) \quad . \tag{1}$$

The error signal $\varepsilon(t)$ is obtained by subtracting the output of the array $S(t)$ from a reference signal $R(t)$.

$$\varepsilon(t) = R(t) - S(t) \quad . \tag{2}$$

The array feedback adjusts the weights w_i to minimize the mean-square value of $\varepsilon(t)$.

In the LMS array, the signal used for the reference $R(t)$ determines which received signals will be accepted by the array and which

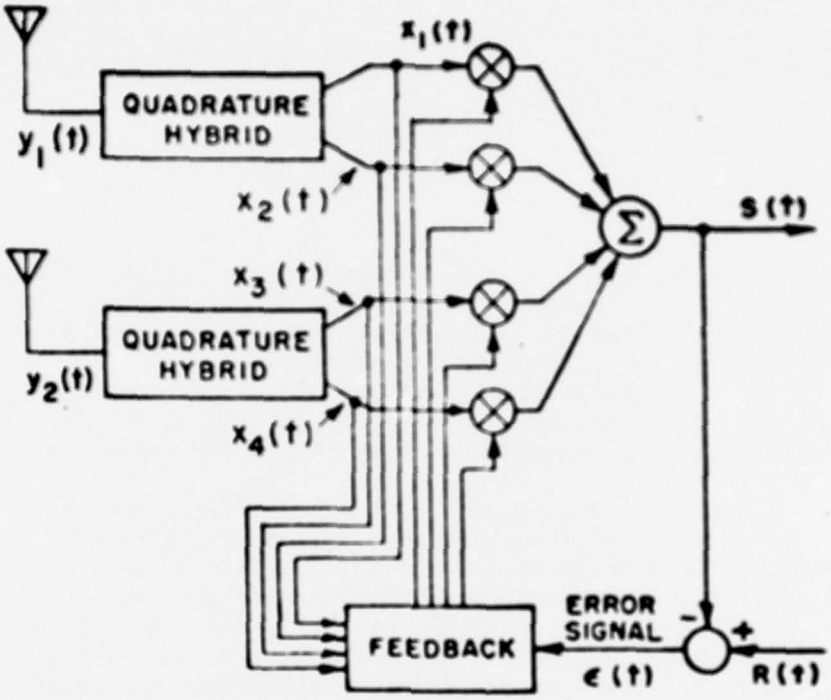

Figure 1. The LMS adaptive array.

will be rejected. When a signal received by the array is highly correlated with the reference signal, the array feedback retains that signal in the output. A signal uncorrelated with the reference signal is nulled by the array. Hence the array can be used to protect a communication system from interference if the reference signal can be made strongly correlated with the desired signal but uncorrelated with the interference. Such a reference signal is usually obtained by processing the array output in some manner that preserves the desired signal but destroys the correlation in the interference components. For this to be possible, it is necessary that the desired signal differ in some known way from the interference.

In Chapter II, we describe a technique for modifying a conventional FM signal so that the array can distinguish between it and the interference. Chapter III describes a method of deriving a reference signal for the adaptive array, based on the signal structure described in Chapter II. Chapter IV discusses the feedback loop bandwidth properties of the LMS algorithm. This information is needed in the following chapter. Chapter V describes the results of some simulations of an adaptive array with the FM signals discussed in Chapter II.

CHAPTER II

A MODIFIED FM SIGNAL

A conventional FM communication signal may be written

$$D(t) = A \cos[\omega_c t + \theta(t)] \tag{3}$$

where A is an amplitude constant, ω_c is the carrier frequency and $\theta(t)$ is a time-varying phase. The instantaneous frequency, ω_i, is

$$\omega_i = \omega_c + \frac{d\theta(t)}{dt} \quad . \tag{4}$$

In ordinary FM, ω_i is linearly related to a modulating signal f(t),

$$\omega_i = \omega_c + K\, f(t) \tag{5}$$

where K is a constant. The signal D(t) then has the form

$$D(t) = A \cos\left[\omega_c t + K \int_0^t f(t')dt' + \theta_o\right] \tag{6}$$

where θ_o is the initial phase at t=0. If, for example, f(t) is sinusoidal at frequency ω_m,

$$f(t) = a \cos \omega_m t \tag{7}$$

the instantaneous frequency ω_i is

$$\omega_i = \omega_c + \Delta\omega \cos \omega_m t \quad . \tag{8}$$

$\Delta\omega$ is called the deviation ($\Delta\omega$ = Ka). The phase variation $\theta(t)$ is

$$\theta(t) = \frac{\Delta\omega}{\omega_m} \sin \omega_m t + \theta_0 \tag{9}$$

and the quantity β,

$$\beta = \frac{\Delta\omega}{\omega_m} \tag{10}$$

is called the modulation index. In general, the bandwidth occupied by the signal increases with β.

We are interested in receiving desired signals of the above type with the adaptive array. To obtain the reference signal-interference signal decorrelation required to allow the adaptive array to null interference, we add an extra phase modulation $\phi(t)$ to this signal. I.e., we suppose the desired signal has the form

$$D(t) = A \cos \left[\omega_c t + K \int_0^t f(t')dt' + \theta_0 + \phi(t) \right] \tag{11}$$

where $\phi(t)$ is a digital waveform with the values 0 and π, on the intervals of length T_ϕ, as shown in Figure 2a. Equation (11) can also be written

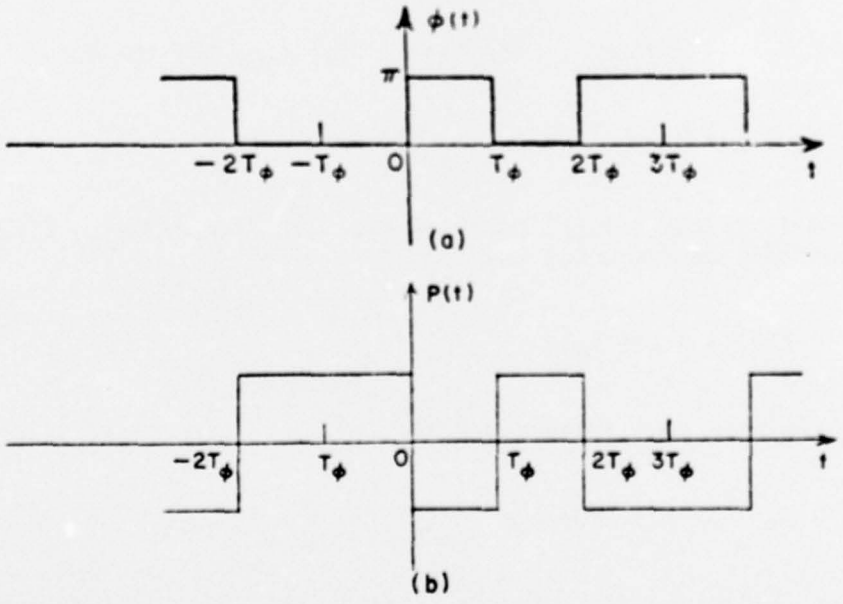

Fiugre 2. (a) The waveform $\phi(t)$; (b) the waveform P(t).

$$D(t) = A\,P(t)\cos\left[\omega_c t + K\int_0^t f(t')dt' + \theta_0\right] \tag{12}$$

where P(t) is a digital waveform with values ±1 as shown in Figure 2b. This modulating waveform P(t) would be added to the desired signal at the transmitter. We obtain the waveform P(t) from a maximal length pseudonoise code generator[4,5]. A typical D(t) is shown sketched in Figure 3c. The modulating signal is assumed to be a sinusoidal waveform (Figure 3a). P(t) in Figure 3b has the effect of changing the sign of the conventional FM signal on a bit interval depending upon the PN sequence.

Since D(t) is the product of a conventional FM signal with P(t), the spectrum of D(t) may be found by convolving the spectra of P(t) and the FM signal. It is apparent that the spectrum of the modified FM signal is spread out depending upon the bandwidth of P(t). To illustrate this point we consider a sinusoidally modulated FM signal of the form

$$d(t) = \cos\left[\omega_c t + \beta \sin \omega_m t\right] \tag{13}$$

and we assume P(t) is a square wave of frequency ω_m. For small modulation index $\beta << \pi/2$, Equation (13) can be written

$$\begin{aligned} d(t) &\cong \cos \omega_c t - \beta \sin \omega_c t \sin \omega_m t \\ &\cong \cos \omega_c t - \frac{\beta}{2}\cos(\omega_c - \omega_m)t + \frac{\beta}{2}\cos(\omega_c + \omega_m)t \quad . \end{aligned} \tag{14}$$

d(t) has the frequency spectrum shown in Figure 4a. The (complex) Fourier coefficients of the square wave are given by

$$C_n = \begin{cases} 0 & n = \text{all even integers} \\ \dfrac{2}{n\pi j} & n = 1,3,5,\cdots \end{cases} \tag{15}$$

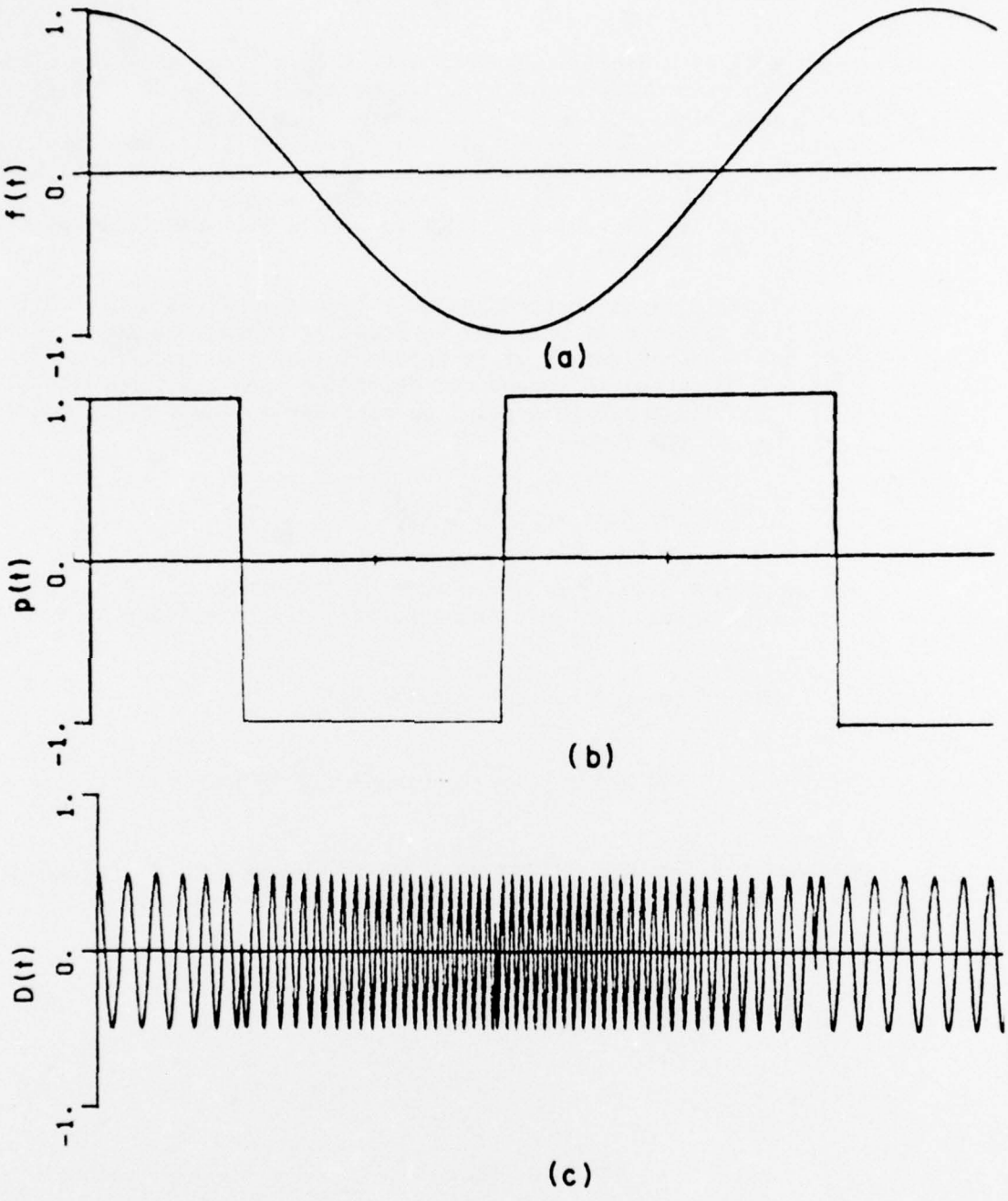

Figure 3. (a) the modulating signal f(t), (b) the PN sequence P(t) and (c) the modified FM signal D(t).

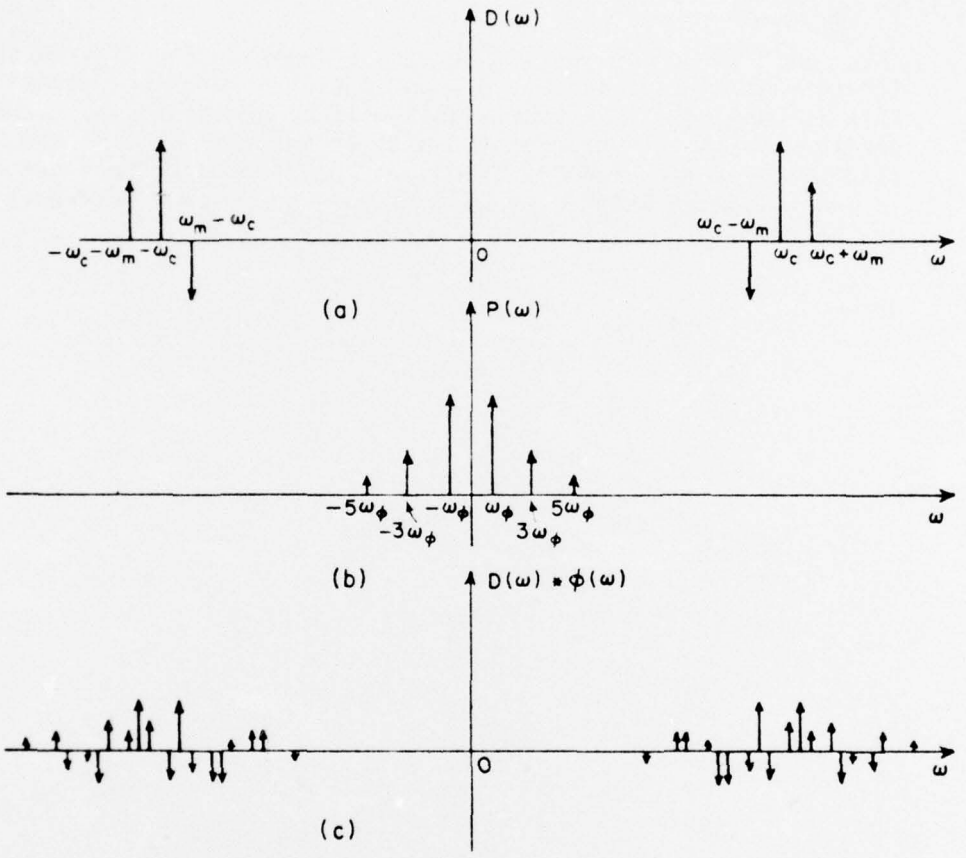

Figure 4. The frequency spectrum of (a) the conventional FM signal d(t), (b) the square wave P(t), and (c) the modified FM signal.

which is plotted as a function of frequency in Figure 4b. To simplify the convolution, three significant pairs of harmonics of $P(\omega)$ have been taken to convolve with $D(\omega)$. We obtain the final spectrum of the modified FM signal in Figure 4c. The presence of $P(t)$ on the desired signal broadens the spectrum of the conventional FM signal. The selection of the bandwidth of $P(t)$ will be discussed in Chapter IV.

With the phase modulation $\phi(t)$ present on the desired signal, the same modulation can be introduced on the reference signal. If this is done, the reference signal will be correlated with the desired signal but uncorrelated with an interference, as long as $\phi(t)$ switches more rapidly than the array feedback loops can track. In the following Chapter we will discuss how such a reference signal can be derived.

CHAPTER III

REFERENCE SIGNAL

Ideally, when the desired signal has the form in Equation (11), the reference signal should also be given by:

$$R(t) = A \cos\left[\omega_c t + K \int_0^t f(t')dt' + \theta_o + \phi(t)\right] \quad , \tag{16}$$

i.e., it must be identical to D(t). The problem, of course, is that f(t) and $\phi(t)$ are not known at the receiving site ahead of time. (If they were, there would be no need for the antenna!) Instead, it is necessary to obtain estimates of f(t) and $\phi(t)$ (which we denote by $\hat{f}(t)$ and $\hat{\phi}(t)$) by demodulating the receiving signal. From these, a reference signal

$$R(t) = A \cos\left[\omega_c t + K \int_0^t \hat{f}(t')dt' + \theta_o + \hat{\phi}(t)\right] \tag{17}$$

may be constructed. This reference signal will be suitable only if f(t) and $\phi(t)$ are sufficiently good estimates of f(t) and $\phi(t)$.

To make use of this technique, it must be possible to demodulate both f(t) and $\phi(t)$ separately, i.e., to extract each waveform without interference from the other. It appears that a Costas loop [6] followed by a baseband delay lock loop[7,8,9] can be used for this purpose. In the following paragraphs we discuss the Costas loop (CL) and the delay lock loop (DLL) respectively and show how the estimates f(t) and $\phi(t)$ may be obtained.

A block diagram of a CL is shown in Figure 5. To understand the operation of this loop, assume that the input is a modified FM signal given by Equation (12)

$$D(t) = A\, P(t) \cos\left[\omega_c t + K \int_0^t f(t')dt'\right] \tag{12}$$

where the initial phase angle θ_o is defined to be zero. The VCO output is split into two quadrature components, $e_1(t)$ and $e_2(t)$, given by

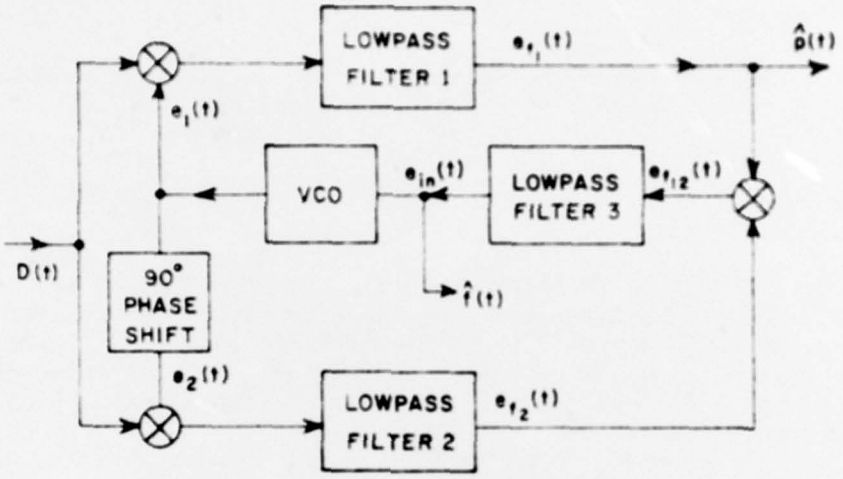

Figure 5. Costas loop.

$$e_1(t) = 2 \cos [\omega_c t + \theta(t)] \tag{18}$$

and

$$e_2(t) = 2 \sin [\omega_c t + \theta(t)] \tag{19}$$

where $\theta(t)$ is a time varying phase angle. The input FM signal is mixed with $e_1(t)$ and $e_2(t)$ separately. The products are passed through the lowpass filters to eliminate the sum output terms from the mixers. The filter outputs become

$$e_{f1}(t) = P(t) \cos\left[K\int_0^t f(t')dt' - \theta(t)\right] \tag{20}$$

and

$$e_{f2}(t) = P(t) \sin\left[K\int_0^t f(t')dt' - \theta(t)\right] \quad . \tag{21}$$

$e_{f1}(t)$ and $e_{f2}(t)$ are then multiplied to give

$$e_{f12}(t) = e_{f1}(t) \cdot e_{f2}(t)$$

$$= \frac{1}{2} P^2(t) \sin 2\left[K\int_0^t f(t')dt' - \theta(t)\right] \quad . \tag{22}$$

The lowpass filter output is

$$e_{in}(t) = \frac{1}{2} \overline{P^2(t)} \sin 2\left[K\int_0^t f(t')dt' - \theta(t)\right]$$

because the filter bandwidth is chosed narrow enough to average $P^2(t)$ but not

$$\sin 2\left[K\int_0^t f(t')dt' - \theta(t)\right] \quad . \tag{23}$$

If the modulation P(t) is ideal, then $P^2(t) = (\pm 1)^2 = 1$ regardless of whether P(t) is +1 or -1, so no filtering is required. However, when the signal in Equation (12) is transmitted through a finite bandwidth, the modulation P(t) produces envelope modulation on D(t) [10] and the lowpass filter is needed to eliminate spikes that will occur in $e_{f12}(t)$.

When the CL is operating in lock, the VCO phase $\theta(t)$ is a good estimate of the input phase deviation. The phase error,

$$K\int_0^t f(t')dt' - \theta(t) \quad ,$$

is small and the VCO input can be approximated by

$$e_{in}(t) \cong K f(t')dt' - \frac{d\theta(t)}{dt} \quad . \tag{24}$$

It is easily seen that this is the desired mode of operation for demodulation of FM. If

$$\theta(t) \approx \int_0^t f(t')dt' \quad ,$$

the VCO frequency is a good estimation of the signal frequency. The signal frequency deviation is proportional to the modulating signal and the VCO frequency is proportional to the signal $e_{in}(t)$. Thus $e_{in}(t)$ is proportional to the signal frequency and can be used as the demodulated output for FM inputs.

Moreover, since

$$\int_0^t f(t')dt' \approx \theta(t),$$

then

$$\cos\left[\int_0^t f(t')dt' - \theta(t)\right] \approx 1 \quad ,$$

so Equation (18) becomes

$$e_{fl}(t) \approx P(t) \tag{25}$$

i.e., $e_{fl}(t)$ is an estimate of the PN code, $P(t)$, on the input signal, $e_{fl}(t) = \hat{P}(t)$. This estimate of $P(t)$, which in general is noisy, can be cleaned up with a delay lock loop, as shown in Figure 6.

Since $P(t)$ is a maximal length PN sequance, the waveform for $P(t)$ is known ahead of time at the receiver. In Figure 6 a generator is used to generate two PN sequences, $P_1(t)$ and $P_2(t)$, which both have the same waveform as $P(t)$ but which differ in timing by one bit interval, i.e., $P_1(t) = P_2(t - T_\phi)$. $\hat{P}(t)$ is mixed with $P_1(t)$ and $P_2(t)$ separately. The products are passed through narrowband filters whose outputs approximate the cross correlation functions of the input signals, that is, $R\hat{p}p_1(\tau)$ and $R\hat{p}p_2(\tau)$. When the DLL is correctly tracking $\hat{P}(t)$, $P_2(t)$ is $P_\phi/2$ ahead of $\hat{P}(t)$ and $P_1(t)$ is $P_\phi/2$ behind $P(t)$. Therefore v_1 and v_2† can be expressed in terms of τ, the time

† strictly speaking, we are referring to the d-c term in v_1 and v_2 here. We do not consider the noise terms (self noise or thermal noise) in the filter output.

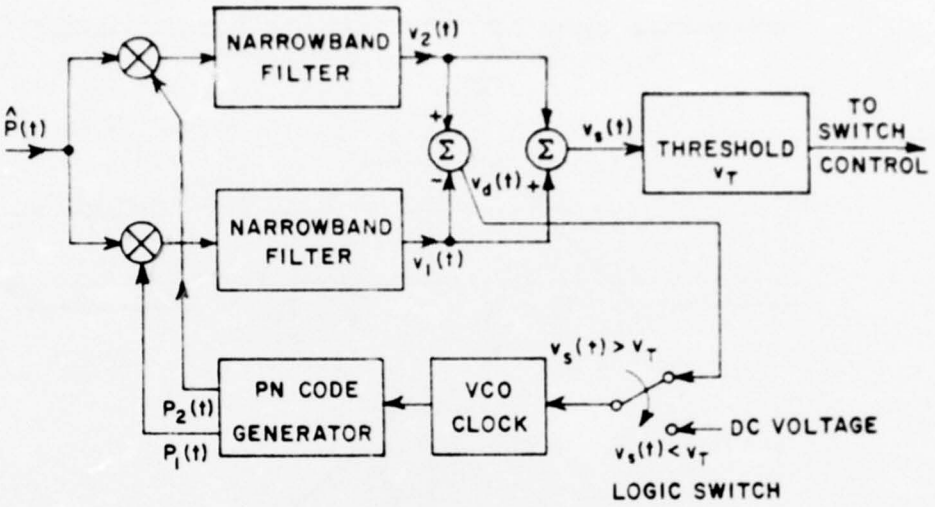

Figure 6. Delay lock loop.

difference between $\hat{P}(t)$ and a code timed half way between $P_1(t)$ and $P_2(t)$. Figure 7a shows $v_1(\tau)$ and $v_2(\tau)$.† The sum and difference of $v_1(\tau)$ and $v_2(\tau)$ are also shown in Figures 7b and 7c respectively. If $v_S(\tau) < v_T$, a fixed DC voltage is connected to the VCO input and drives the VCO at a pre-determined speed until the timing of the generated PN sequences and $P(t)$ is close ($v_S(\tau) > v_T$). The VCO input is then switched to the difference voltage v_d which tends to drive the DLL into lock.

By utilizing the Costas loop and delay lock loop together we can obtain estimates of the modulating signal $f(t)$ and the PN coded signal $P(t)$. A reference signal for the array can then be generated as shown in Figure 8. When the DLL is locked, its output code timing

---

† The autocorrelation function of a maximal length PN sequency is derived in [5].

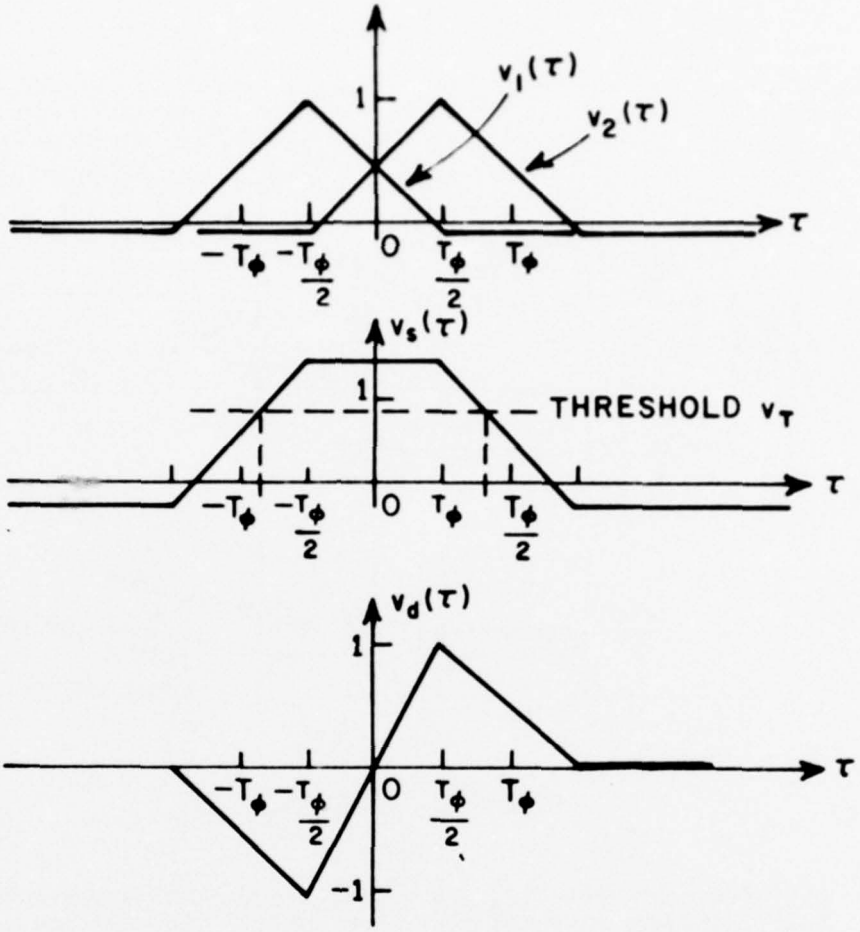

Figure 7. (a) The waveforms $v_1(\tau)$ and $v_2(\tau)$. (b) The sum $v_S(\tau)$ and (c) the difference of $v_1(\tau)$ and $v_2(\tau)$.

is $P_\phi/2$ off from the desired signal code. To compensate for this time difference, a time shift of $P_\phi/2$ is included in Figure 8. It is also noted that there will be a time delay between $\hat{f}(t)$ and $f(t)$ due to the filtering in the Costas loop. To maintain correlation between the reference signal and the desired signal, this time delay must be minimized. The effect of this delay on array performance is studied in Chapter V.

In addition to using the reference signal as derived in Figure 8, another approach is to simply not include the FM modulation in the reference signal. Instead, a signal of the form

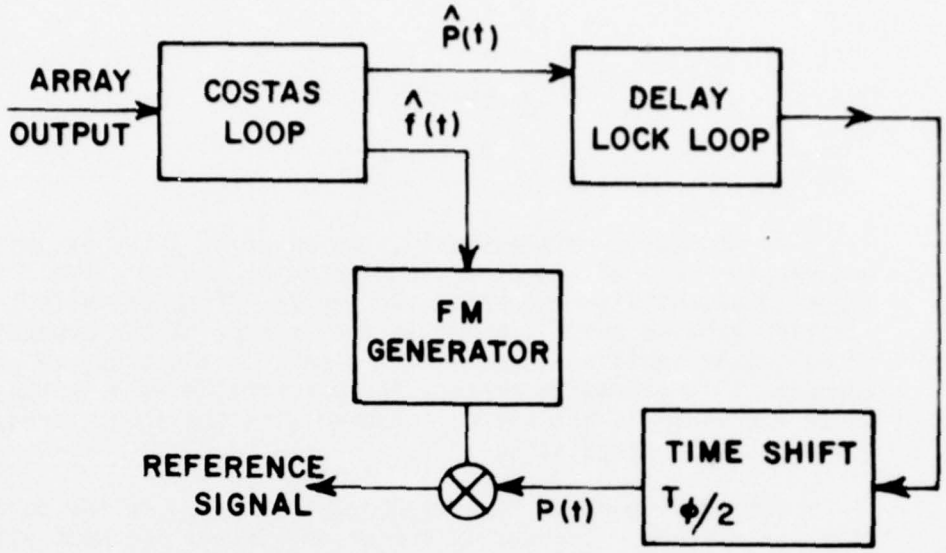

Figure 8. Reference signal generation loop.

$$R(t) = A \cos [\omega_c t + \hat{\phi}(t)] \tag{26}$$

could be used. This eliminates the problem of time delay between $f(t)$ and $f(t)$, but we suspect that this approach is suitable only if the frequency deviation of the modulation term

$$\int_0^t f(t')dt'$$

in the desired signal is small, i.e., only for low values of modulation index. Chapter V also discusses this type of reference signal and shows what performance may be expected.

CHAPTER IV

THE LMS LOOP

As we mentioned previously, the adaptive array discriminates between the desired signal and the interference by correlating the incoming signal with the reference signal. Theoretically the correlation between these signals is the average of the product of the signals over an infinite period of time. In the adaptive array, however, this averaging process is approximated by a lowpass filter whose bandwidth is set narrow compared with the lowest frequency of the baseband desired signal.

The LMS algorithm is a feedback rule based on the method of steepest descent. Changes in the weight vector are made along the direction of the estimated gradient vector. The weight control equation is (1,2):

$$\frac{d}{dt} W(t) = -k_A \nabla_W [\epsilon^2(t)] \tag{27}$$

where W(t) is a column vector whose components are the array weights,

$$W(t) = \begin{pmatrix} w_1(t) \\ w_2(t) \\ w_3(t) \\ w_4(t) \end{pmatrix} , \tag{28}$$

k_A is a positive constant which we refer to as the loop gain constant and $\nabla_W[\epsilon^2(t)]$ is the estimated gradient vector of the mean-square error with respect to W. Equation (27) can be written

$$\frac{d}{dt} W(t) = 2 k_A \epsilon(t) X(t) \tag{29}$$

where X(t) is the signal-input vector,

$$X(t) = \begin{pmatrix} x_1(t) \\ x_2(t) \\ x_3(t) \\ x_4(t) \end{pmatrix} \quad . \tag{30}$$

(Note that the input signal components, such as $x_1(t)$, each consist of three components, the desired signal, the interference and thermal noise.) Equation (29) can also be written in its integral form

$$W(t) = W_i(0) + 2\, k_A \int_{t'=0}^{t} X(t')\, \varepsilon(t')dt' \tag{31}$$

where $W_i(0)$ is the initial weight vector. Thus we see that each weight, w_i, is obtained by integrating the product of $x_i(t)$ and $\varepsilon(t)$. A circuit implementation of Equation (31) is described in [2].

If we substitute Equation (2) into Equation (29) and define matrices S and Φ as follows:

$$S(t) = R(t)\, X(t) \quad , \tag{32}$$

and

$$\Phi(t) = \begin{pmatrix} x_1(t)x_1(t) & x_1(t)x_2(t) & x_1(t)x_3(t) & x_1(t)x_4(t) \\ x_2(t)x_1(t) & x_2(t)x_2(t) & x_2(t)x_3(t) & x_2(t)x_4(t) \\ x_3(t)x_1(t) & x_3(t)x_2(t) & x_3(t)x_3(t) & x_3(t)x_4(t) \\ x_4(t)x_1(t) & x_4(t)x_2(t) & x_4(t)x_3(t) & x_4(t)x_4(t) \end{pmatrix} , \tag{33}$$

then the system of differential equations of the weights can be expressed as

$$\frac{d}{dt}\, W(t) + 2\, k_A\, \Phi(t)\, W(t) = 2\, k_A\, S(t) \quad . \tag{34}$$

This equation represents the operation of a (multidimensional) lowpass filter on S(t). It is a coupled system of differential equations with time varying coefficients. An exact solution in the general case is

difficult to obtain. However, various techniques[11,12,13] have been used to obtain meaningful approximate solutions. Here we assume the frequency components other than the dc term can be neglected and thus $\Phi(t)$ is approximately a constant matrix. With constant Φ, it is easy to uncouple the system (34) and to obtain its solutions.

An orthogonal matrix, P, is chosen to diagonalize Φ, i.e.,

$$P^T \Phi P = \Lambda = \begin{pmatrix} \lambda_1 & & & 0 \\ & \lambda_2 & & \\ & & \lambda_3 & \\ 0 & & & \lambda_4 \end{pmatrix} \tag{35}$$

where λ_1 to λ_4 are eigenvalues. We define a transformed weight vector $\eta(t)$:

$$\eta(t) = P^{-1} W = \begin{pmatrix} \eta_1(t) \\ \eta_2(t) \\ \eta_3(t) \\ \eta_4(t) \end{pmatrix} . \tag{36}$$

Applying Equations (35) and (36) to Equation (34), we obtain the uncoupled system

$$\frac{d}{dt} \eta(t) + 2 k_A \Lambda \eta(t) = 2 k_A P^T S(t) . \tag{37}$$

The solutions are given by

$$\eta_i(t) = \frac{q_i}{\lambda_i} + \left[\eta_i(0) - \frac{q_i}{\lambda_i} \right] e^{-2k_A \lambda_i t} \tag{38}$$

where $\eta_i(0)$ denotes the initial value of $\eta_i(t)$ and q_i is the ith component of the column vector

$$Q = P^T S = \begin{pmatrix} q_1(t) \\ q_2(t) \\ q_3(t) \\ q_4(t) \end{pmatrix} \quad . \tag{39}$$

When Equation (36) is used to calculate the weights w_i from these $n_i(t)$, we find that each w_i will consist of a sum of exponentials with time constants

$$\tau_i = \frac{1}{2k_A \lambda_i} \quad . \tag{40}$$

Note that the speed of response of the array is limited by the smallest eigenvalue of Φ in Equation (35). We therefore define the time constant of the array to be

$$\tau = \frac{1}{2k_A \lambda_{min}} \tag{41}$$

where

$$\lambda_{min} = \min_j \{\lambda_j\} \quad . \tag{42}$$

We also note that the bandwidth of the lowpass filter described in Equation (34) is determined by the largest eigenvalue of Φ and thus the feedback loop bandwidth is defined by

$$B.W. = 2\ k_A\ \lambda_{max} \tag{43}$$

where

$$\lambda_{max} = \max_j \{\lambda_j\} \quad . \tag{44}$$

Each weight has a dc term and a fluctuating component which result, respectively, from the dc term in $R(t)X(t)$ and the difference frequency

terms in $R(t)X(t)$.* It is clear that spectral components of $2k_A R(t)X(t)$ above the cutoff frequency $2k_A\lambda_{max}$ have little effect on the weights. On the other hand, dc components of $2k_A R(t)X(t)$ determine the dc values of the weights, and non-zero frequency components of $2k_A R(t)X(t)$ below the cutoff frequency $2k_A\lambda_{max}$ produce weight fluctuation or jitter.

In a radio communication system the signals $x_i(t)$ and $R(t)$ are bandlimited with spectral components confined to some region around a carrier frequency. The carrier frequency is assumed to be high compared to the bandwidth. Thus the product $R(t)x_i(t)$ contains power in a band around zero frequency and also in a band around twice the carrier frequency. When the reference signal is properly designed, the desired signal-reference signal product in $R(t)x_i(t)$ contributes a large dc term that determines the steady state weights and causes the array to retain the desired signal in the array output. The interference signal-reference signal should have no dc term and should have as little power as possible within the feedback bandwidth, $2k_A\lambda_{max}$. When this is the case, the array nulls the interference. Thus we say that, in the adaptive array sense, two signals are strongly "correlated" when most of the power in the spectral products they contribute to $R(t)x_i(t)$ lies within the feedback loop bandwidth, $2k_A\lambda_{max}$. On the other hand, two signals are "uncorrelated" as long as the power in these spectral components is mostly outside the loop bandwidth.

As we discussed in Chapters II and III, the proper desired signal correlation and interference decorrelation can be achieved by the introduction of a phase switching in the desired and reference signals. Accordingly, the choice of the feedback loop bandwidth and the code frequency** (f_ϕ) must be compatible. In the following paragraphs the design tradeoff between these parameters is discussed.

Since the desired signal is transmitted through a finite bandwidth, the modulation $P(t)$ produces envelope distortion on $D(t)$, especially in the region of a bit transition where the envelope rolls over[10]. The slope at which the envelope rolls over is determined by the system bandwidth but not by the code frequency. To minimize envelope distortion we could broaden the system bandwidth. However, our goal here is to transmit the signal in Equation (11) through a conventional FM bandwidth. For that reason, we choose the code frequency near the low end of the audio band,

---

* The difference frequency terms in Φ also contribute to the fluctuating component of each weight.

**The code frequency is $f_\phi = T_\phi^{-1}$, where T_ϕ is the bit interval.

$$f_{\phi} \approx f_{min} \tag{45}$$

where f_{min} is the lowest audio frequency component in the modulation, for example, 100 Hz.

On the other hand the feedback loop bandwidth has to be narrow compared with f_{ϕ}. Otherwise the array weights will track the switching of the biphase modulation and could modulate a CW interference signal to make it match the biphase modulated reference signal. Then the decorrelation between I(t) and R(t) will not occur. Hence

$$\text{B.W.} = 2k_A\lambda_{max} << 2\pi f_{\phi} \quad . \tag{46}$$

In addition, to prevent the array weights from responding to the audio modulation, we also want

$$\text{B.W.} = 2k_A\lambda_{max} << 2\pi f_{min} \quad . \tag{47}$$

Combining Equations (46) and (47), we have

$$\text{B.W.} = 2k_A\lambda_{max} << \min \{2\pi f_{\phi}, 2\pi f_{min}\} \quad . \tag{48}$$

It is clear that the eigenvalues λ_j depend upon the power of the incoming signals. (See Equation (33).) The bandwidth of the feedback loop is proportional to λ_{max}, which is determined by the strongest interference signal. The array has to be designed to operate over a range of signal powers. Thus the loop gain constant $2k_A$ must be chosen to enforce the inequality (48) for the strongest I(t) to be received.

CHAPTER V

RESULTS

In this chapter we study the performance of a two element adaptive array with two different types of reference signals, as discussed in Chapter III. First, the reference signal is assumed to be obtained by processing the array output as shown in Figure 8. Then, a simpler reference signal as in Equation (26) is assumed, i.e., the FM modulation is not included. We consider only the case where the interference is a CW signal and the desired signal is a coded FM signal with CW modulation.

The desired signal is assumed to arrive at the array from an angle θ_d (see Figure 9) producing element signals

$$y_{1d}(t) = A \sin [\omega_d t + \beta \sin \omega_m t + \phi(t)] \tag{49}$$

and

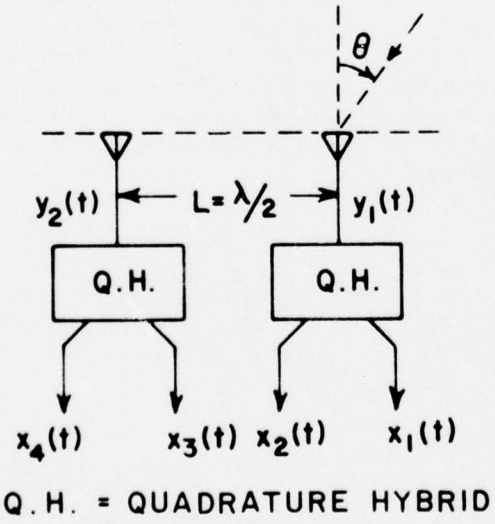

Figure 9. A two-element array.

$$y_{2d}(t) = A \sin [\omega_d t + \beta \sin \omega_m t + \phi(t) - \gamma_d] \quad , \tag{50}$$

where

$$\gamma_d = \frac{2\pi L}{\lambda_d} \sin \theta_d \quad , \tag{51}$$

L is the spacing between elements, which is assumed a half wavelength at frequency ω_d. λ_d is the free-space wavleength at frequency ω_d, A is amplitude constant, β is the modulation index, and ω_m is the modulating frequency. The subscript "d" denotes the desired signal portion of $y_1(t)$ and $y_2(t)$.

In order to study the effects of Doppler shift or transmitter frequency inaccuracies, we assume the desired carrier ω_d varies around a fixed frequency ω_c. We refer to this variation as the frequency offset and define the percentage frequency offset by

$$\% \text{ frequency offset} = \frac{\omega_d - \omega_c}{\omega_c} \times 100 \quad . \tag{52}$$

As discussed in Chapter III, the reference signal code will be generated by a delay lock loop. In general, because of tracking inaccuracies, a time difference τ may exist between the codes in the desired signal and the reference signal. This time difference is referred to as code timing offset. We define the percentage code timing offset by

$$\% \text{ code timing offset} = \frac{\text{time difference } \tau}{\text{bit interval } T_\phi} \times 100 \quad . \tag{53}$$

The effect of code timing offset on the array performance will also be studied.

The interference signal is assumed to propagate into the array from an angle θ_i, producing element signals (see Figure 9)

$$y_{1i}(t) = B \sin \omega_i t \tag{54}$$

and

$$y_{2i}(t) = B \sin (\omega_i t - \gamma_i) \quad , \tag{55}$$

where

$$\gamma_i = \frac{2\pi L \sin \theta_i}{\lambda_i} \quad , \tag{56}$$

B is an amplitude constant and λ_i is the free-space wavelength* at frequency ω_i. The subscript "i" denotes the interference signal portion of $y_1(t)$ and $y_2(t)$. In the results described below, ω_i will be assumed equal to ω_c, i.e., the interference signal is exactly on on the desired signal design frequency.

The total element signals are

$$y_1(t) = y_{1d}(t) + y_{1i}(t) \tag{57}$$

and

$$y_2(t) = y_{2d}(t) + y_{2i}(t) \quad . \tag{58}$$

The inphase and quadrature components (see Figure 9) are thus

$$x_1(t) = A \sin [\omega_d t + \beta \sin \omega_m t + \phi(t)] + B \sin \omega_c t \tag{59}$$

$$x_2(t) = A \cos [\omega_d t + \beta \sin \omega_m t + \phi(t)] + B \cos \omega_c t \tag{60}$$

$$x_3(t) = A \sin [\omega_d t + \beta \sin \omega_m t + \phi(t) - \gamma_d] + B \sin(\omega_c t - \gamma_i) \tag{61}$$

and

$$x_4(t) = A \cos [\omega_d t + \beta \sin \omega_m t + \phi(t) - \gamma_d] + B \cos(\omega_c t - \gamma_i) \quad . \tag{62}$$

---

* This λ_i has no relation to the eigenvalues λ_i discussed in Chapter IV.

In the results described below, A is set equal to 1 and B=10. This choice makes the input signal-to-interference ratio -20 dB. Furthermore we assume $\theta_d = 0°$ and $\theta_i = 60°$.

With the input signals defined above, we will discuss the array performance with the two kinds of reference signals in the following sub-sections, A and B. The results in sub-section A will be based on theoretical derivations while those in sub-section B will also utilize simulation results.

A. Reference Signal with FM Modulation

In this sub-section the reference signal has the form

$$R(t) = A \sin [\omega_c t + \beta \sin \omega_m (t-t_o) + \phi(t-\tau)] \tag{63}$$

where it is assumed that the Costas loop preserves the exact waveform of the modulating signal but its output is delayed by a time t_o, and also the code timing is offset by a time τ.

To evaluate the array performance with this type of reference signal we first calculate the steady state weights that will result. The steady-state weights are given by[2]

$$W_{ss} = \begin{pmatrix} W_{ss1} \\ W_{ss2} \\ W_{ss3} \\ W_{ss4} \end{pmatrix} = \Phi^{-1} S \tag{64}$$

where

$$\Phi = \begin{pmatrix} \overline{X_1(t)X_1(t)} & \overline{X_1(t)X_2(t)} & \overline{X_1(t)X_3(t)} & \overline{X_1(t)X_4(t)} \\ \overline{X_2(t)X_1(t)} & \overline{X_2(t)X_2(t)} & \overline{X_2(t)X_3(t)} & \overline{X_2(t)X_4(t)} \\ \overline{X_3(t)X_1(t)} & \overline{X_3(t)X_2(t)} & \overline{X_3(t)X_3(t)} & \overline{X_3(t)X_4(t)} \\ \overline{X_4(t)X_1(t)} & \overline{X_4(t)X_2(t)} & \overline{X_4(t)X_3(t)} & \overline{X_4(t)X_4(t)} \end{pmatrix} \tag{65}$$

and

$$S = \begin{pmatrix} \overline{R(t)X_1(t)} \\ \overline{R(t)X_2(t)} \\ \overline{R(t)X_3(t)} \\ \overline{R(t)X_4(t)} \end{pmatrix} \quad , \tag{66}$$

where the overbar denotes an infinite time average. Thus all frequency components of $\overline{x_i(t)x_j(t)}$ in S are dropped except the dc terms. From W_{SS}, the output power of the desired signal and the interference can be found and thus the output signal-to-interference ratio is obtained.

Consider first the case where the coded PN sequence is assumed synchronized at the receiver, i.e., $\tau=0$. The reference signal then becomes

$$R(t) = A \sin [\omega_c t + \beta \sin \omega_m (t-t_o) + \phi(t)] \quad . \tag{67}$$

It is shown in Appendix A that the steady state weight vector in this case is given by

$$W_{SS} = \begin{pmatrix} .5 \\ -.1068 \\ .5 \\ .1068 \end{pmatrix} J_o\left(2\beta \sin \frac{\omega_m t_o}{2}\right) \tag{68}$$

where $J_o(X)$ is the Bessel function of order zero. We see that the weights all contain the factor

$$J_o\left(2\beta \sin \frac{\omega_m t_o}{2}\right)$$

so the absolute magnitude of the array response will vary with β and t_o according to

$$J_o\left(2\beta \sin \frac{\omega_m t_o}{2}\right) \quad ,$$

but there will be no change in pattern (relative response versus angle) with t_o or β. This result is understandable since changing β and t_o does not change ϕ. Moreover, the reference signal R(t) can be written in the form

$$R(t) = \alpha_1 R_1(t) + \alpha_2 R_2(t) \tag{69}$$

where $R_1(t)$ is perfectly correlated with the desired signal and $R_2(t)$ is uncorrelated with the desired signal. Increasing β or t_o increases α_2 and decreases α_1.

The resulting attenuation of the desired signal (which is denoted by ADS) is plotted in Figure 10 versus the modulation phase delay ($\omega_m t_o/2$) with β as a parameter. When β is small ($\beta << \pi/2$), the narrowband FM signal has most of its power concentrated in the carrier. The desired signal is highly correlated with the reference signal regardless of t_o and thus ADS is negligible for all t_o. When ($\beta < \pi/2$), ADS becomes significant. At some values of t_o, there is no correlation between the desired and reference signals at all. Therefore the output desired signal power is zero.

Theoretically, because of the PN coded phase modulation on the desired and reference signals, the infinite time average of the products of I(t)R(t) and I(t)D(t) is zero.* There is no interference power at the array output.

The above results indicate that to maintain low ADS, the modulation delay must be minimized. For small modulation index β, the requirement on t_o can be eased. If, for example, a system can tolerate 10 dB attenuation on the desired signal, and β=1, the modulation delay cannot exceed one tenth of the minimum audio cycle.** If β=1, the limit on t_o is one quarter of the minimum audio cycle.

Now we consider the opposite case where there is no modulation delay, i.e., t_o=0, but there is code delay τ. The reference signal is

---

* See the footnote on Page 57.

**The modulating signal we envision is an audio signal whose maximum frequency component gives the minimum audio cycle.

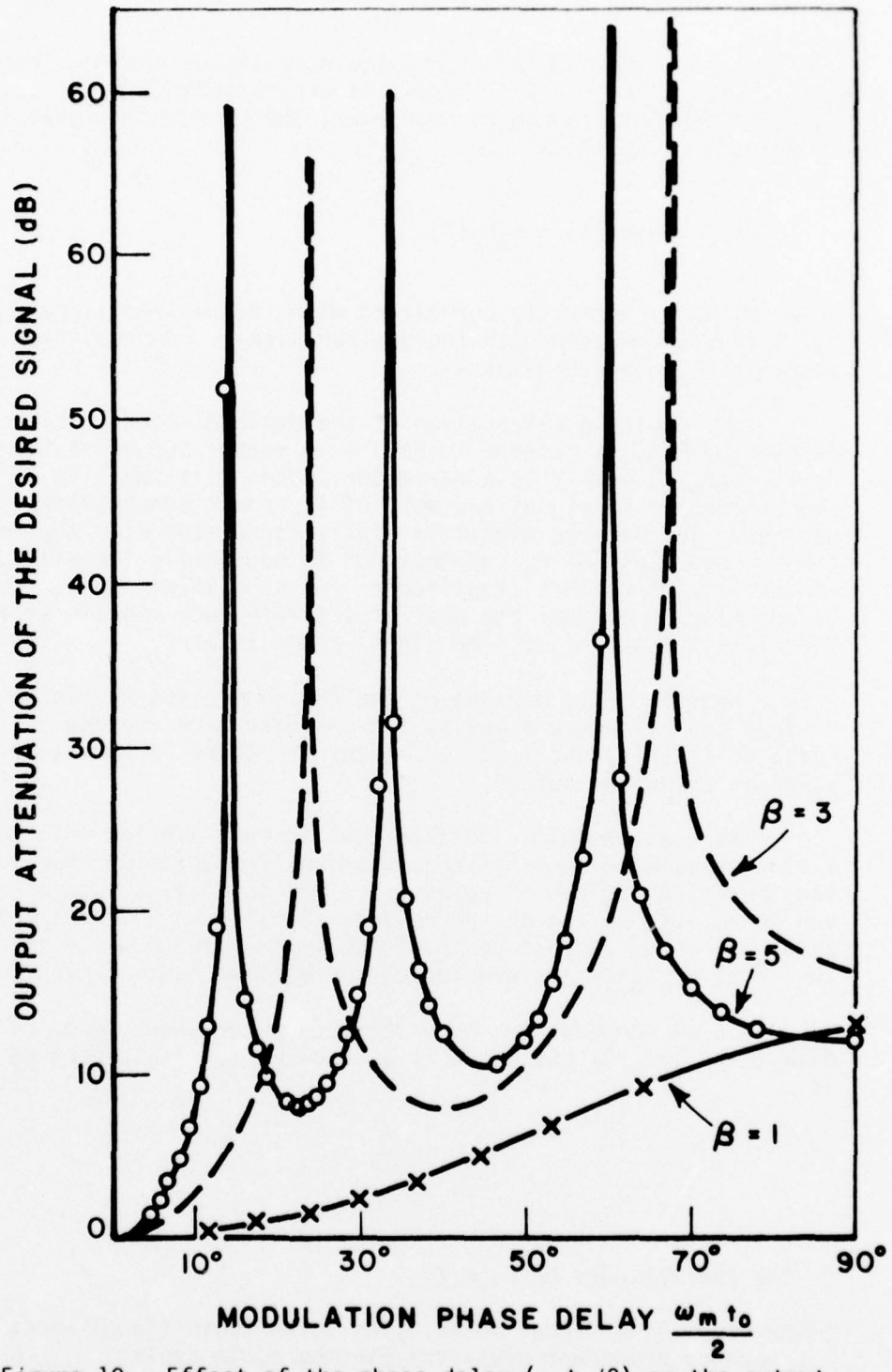

Figure 10. Effect of the phase delay ($\omega_m t_o/2$) on the output desired signal attenuation.

$$R(t) = A \sin [\omega_c t + \beta \sin \omega_m t + \phi(t-\tau)] \quad . \tag{70}$$

In this case the steady state weight vector is found in Appendix B to be

$$W_{ss} = \begin{pmatrix} .5 \\ -.1068 \\ .5 \\ .1068 \end{pmatrix} R_p(\tau) \tag{71}$$

where $R_p(\tau)$ is the autocorrelation function of the PN code. For a PN sequence of long period, $R_p(\tau)$ can be approximated by

$$R_p(\tau) = \begin{cases} 1 - \frac{\tau}{T_\phi} & 0 \leq \tau \leq T_\phi \\ 1 + \frac{\tau}{T_\phi} & -T_\phi \leq \tau \leq 0 \\ 0 & \text{elsewhere} \end{cases} \quad . \tag{72}$$

The steady state weight vector in Equation (71) is a product of a column vector and a factor $R_p(\tau)$. This column vector is shown in Appendix B to be a function of the signal amplitudes and arrival angles which are assumed constant in this case. Hence the array pattern is fixed for all τ. However, the absolute magnitude of the array response varies with the code timing offset since τ affects the correlation between the desired and reference signals. Note that β is not a parameter here because we assume the FM modulation in the reference signal to be perfect.

The attenuation of the desired signal versus the percentage code timing offset is shown in Figure 11. It is seen that the ADS increases as the code timing offset increases. When the timing is offset by one bit interval, there is no correlation between the desired and reference signals. Thus the desired signal is attenuated infinitely by the array.

The theoretical results based on an infinite time average show that the interference signal in this case is not correlated with the

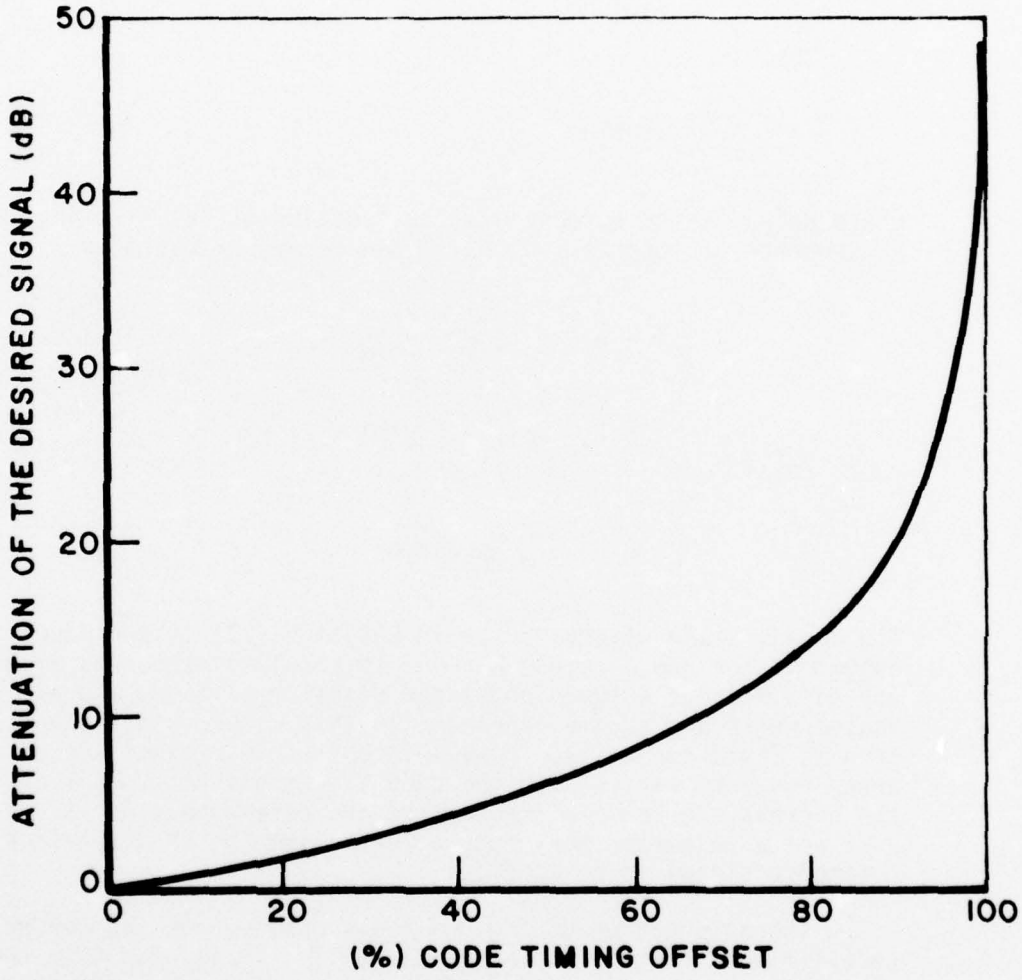

Figure 11. Effect of the code timing offset on the output desired signal attenuation.

reference signal at all.* Therefore the array nulls out the interference signal completely.

From Figure 11, it is seen that the code timing offset must be kept small for satisfactory array performance. In the delay lock loop, the code timing tracking error must be kept less than 68% of a bit interval if 10 dB desired signal attenuation can be tolerated in a system.

In the next sub-section, we examine the performance of the array when the reference signal does not contain the FM modulation.

B. Reference Signal Without FM Modulation

In this sub-section the performance of the adaptive array is studied when the reference signal is a simple bi-phase modulated signal of the form

$$R(t) = A \sin [\omega_R t + \phi(t-\tau)] \quad , \tag{73}$$

where the frequency ω_R is equal to ω_C, $\phi(t-\tau)$ is a PN sequance which has the same waveform as that in the desired signal except for the time difference τ. For simplicity, in this sub-section we assume $\phi(t)$ to be a square wave at frequency ω_ϕ. The incoming signals are defined in Equations (59) to (62).

To study the array performance with the reference signal given above, the LMS algorithm is utilized to find the approximate solutions to Equation (64). The discrete form of the LMS algorithm is simulated on the computer for this purpose. Each weight is adjusted according to the rule[1]

$$w_i(j+1) = w_i(j) - 2k_D \varepsilon(j) x_i(j) \tag{74}$$

where j is the sample index and k_D is the digital feedback loop gain constant. k_D is chosen so the digital feedback loop is stable and has the lowpass filter characteristics as discussed in Chapter IV. The relation between k_D and the analog loop gain constant k_A has been found[10] to be

---

* See the footnote on page 57.

$$k_D = \frac{1 - e^{-2k_A \lambda_{max} T_S}}{2\lambda_{max}} \tag{75}$$

where T_S is the sampling period. From k_D the digital feedback loop bandwidth and its time constant are[10]

$$B_D = \frac{-\ln(1-2k_D\lambda_{max})}{T_S} \tag{76}$$

and

$$\tau_D = \frac{-T_S}{\ln(1-2k_D\lambda_{min}} \quad . \tag{77}$$

Unfortunately, if typical design frequencies are used with this digital algorithm, excessive computer time is needed before the weights reach the steady state. For example, consider f_{min}=100 Hz, $f_d=f_j$=10 MHz, $T_S=2.5\ 10^{-8}$, A=1, B=10, $\theta_d=0°$, $\theta_j=60°$. The maximum and minimum eigenvalues of the covariance matrix in Equation (65) can be shown to be*

$$\begin{matrix}\lambda_{max} \\ \lambda_{min}\end{matrix} = (A^2 + B^2) \pm \sqrt{A^4 + B^4 + 2A^2B^2 \cos\pi \left(\sin\theta_d - \frac{f_j}{f_d} \sin\theta_j\right)} \quad . \tag{78}$$

With numerical values substituted into Equation (78) we have λ_{max}=200 and λ_{min}=2. Satisfying the bandwidth requirements of Equation (48) gives

$$B_D << 2\pi f_{min} = 2\pi 100 \quad . \tag{79}$$

For $B_D = 2\pi 10$, we find $k_D = 3.927 \times 10^{-9}$ and $\tau_D = 6.3694 \times 10^7\ T_S$.

---

* The matrix Φ that results for the signals defined in Equations (59) to (62) is derived in Appendix A, Equation (85).

Hence for the digital array the response time (say 5 time constants) is 3.1847×10^8 iterations. With the size of the computer program needed in this simulation (each iteration requires about 3.6×10^{-3} seconds), impractically long computer running times result. In order to increase the simulation speed, large values of k_D and scaled frequencies must be used. However, large values of k_D result in a wider feedback loop bandwidth. A compromise is made on f_{min} and f_i to satisfy the bandwidth requirement in Equation (48). Thus, in these simulations, we choose f_{min} = 4 KHz, $\omega_c = \omega_d = \omega_i = \omega_R$ = 455 KHz, k_D = .00005, $T_S = 2.1978 \times 10^{-7}$ seconds, $B_D = 2\pi(1.45 \times 10^3)$ rad/sec and $\tau_D = 50000T_S$. With these choices the computer time is greatly reduced and the inequality (48) is still met. The corresponding analog time constant in the real array is found by Equations (41) and (75) to be .01098 seconds.

The initial values of the weights are chosen to be

$$W(0) = \begin{pmatrix} 1 \\ 0 \\ 0 \\ 0 \end{pmatrix} . \qquad (80)$$

At the beginning of the simulation, each weight in the array goes through a transient. After the weight transient has ended, and the weights have become stationary, m successive samples* of each weight are stored on a magnetic tape. From these weights, the average output power of the interference or the desired signal is calculated.

A computer program has been written to perform the tedious calculations. The values of the modulation index β, the code timing offset τ and the desired carrier frequency offset can be varied so that their effects on the array performance can be studied.

---

* The steady state array weights have fluctuating components due to the spectral lines of the products, I(t)R(t) and D(t)R(t). The value of m is so chosen that m samples form a suitable average over these fluctuations.

First, we consider the transient pattern behavior of the array. We assume that $\beta = 1.2$, $f_\phi = 20$ KHz and that there is no frequency offset or code timing offset. The reference signal is given in Equation (73). The starting weight vector has been set equal to W(0) (Equation (80)), so the initial pattern is omnidirectional. A desired signal is assumed incident on the array from broadside ($\theta_d=0°$) and an interference signal from $\theta_i=60°$. The results are shown in Figures 12-17. Figure 12 shows the initial pattern. Figure 13 shows the pattern after 2 time constants, and so forth, up to Figure 16 which shows the pattern after 4 time constants. Figure 17 shows the steady state pattern at $t\to\infty$. It can be seen that the final array response is about 65 dB weaker in the interference direction than in the desired signal direction. Note that the input signal-to-interference ratio is -20 dB. Figure 18 shows the transient behavior of the array weights.

Figures 19a and 19b show the steady-state attenuation of the desired signal (ADS) and the output signal-to-interference ratio (SIR), respectively, as a function of the modulation index β with the code frequency f_ϕ as a parameter. The input signals are defined in Equations (59) to (62). The reference signal is given above. We assume the code timing is synchronized at the receiver ($\tau=0$) and there is no frequency offset, $\omega_d=\omega_i=\omega_R=455$ KHz. In Figure 19a the ADS is plotted versus β. The data shown have been obtained three different ways. First, the solid curve has been obtained from theoretical calculations. These calculations are contained in Appendix D. Next, the points marked as "x" and "o" have been obtained by computer simulations of the LMS loop, whose bandwidth is fixed at $2\pi(1.45 \times 10^3)$ rad/sec. The x's are obtained with $f_\phi = 20$ KHz and the o's with $f_\phi = 200$ Hz. It is seen that regardless of the switching frequency f_ϕ, the theoretical ADS agrees closely with the simulated values. This is understandable because the correlation between the desired and the reference signal is independent of f_ϕ. The theoretical steady state weight vector is found in Appendix D to be

$$W_{SS} = \begin{pmatrix} .5 \\ -.1068 \\ .5 \\ .1068 \end{pmatrix} J_0(\beta) \quad . \tag{81}$$

The absolute magnitude of the array response is scaled by the factor $J_0(\beta)$ but β does not affect the relative array pattern. β changes the correlation between the desired and reference signals and the result is that all the weights are scaled by the factor $J_0(\beta)$. At some particular values of β, which decorrelate R(t) and D(t) completely, the weights become zero and hence ADS becomes infinite.

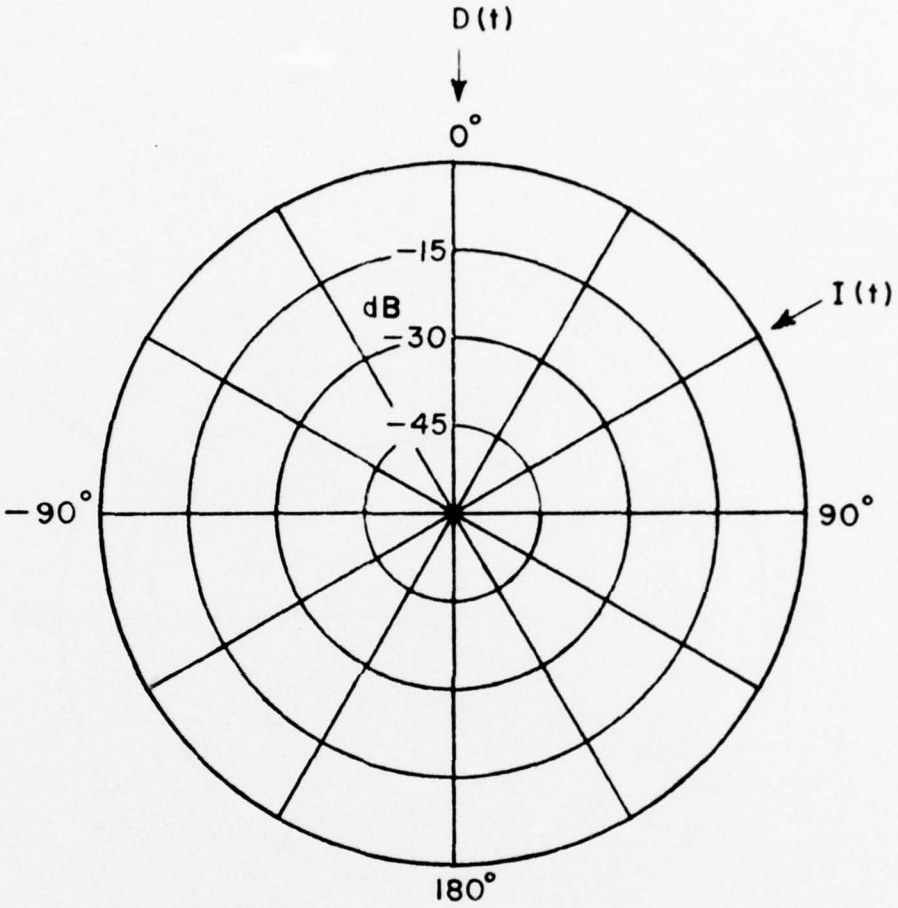

Figure 12. Initial omnidirectional pattern.
Pattern computer at f=455 KHz.
β = .1
k_D = .000005
$(S/I)_m$ = -20 dB
θ_i = 60°
θ_d = 0°
f_m = 4 kHz
f_ϕ = 20 kHz.

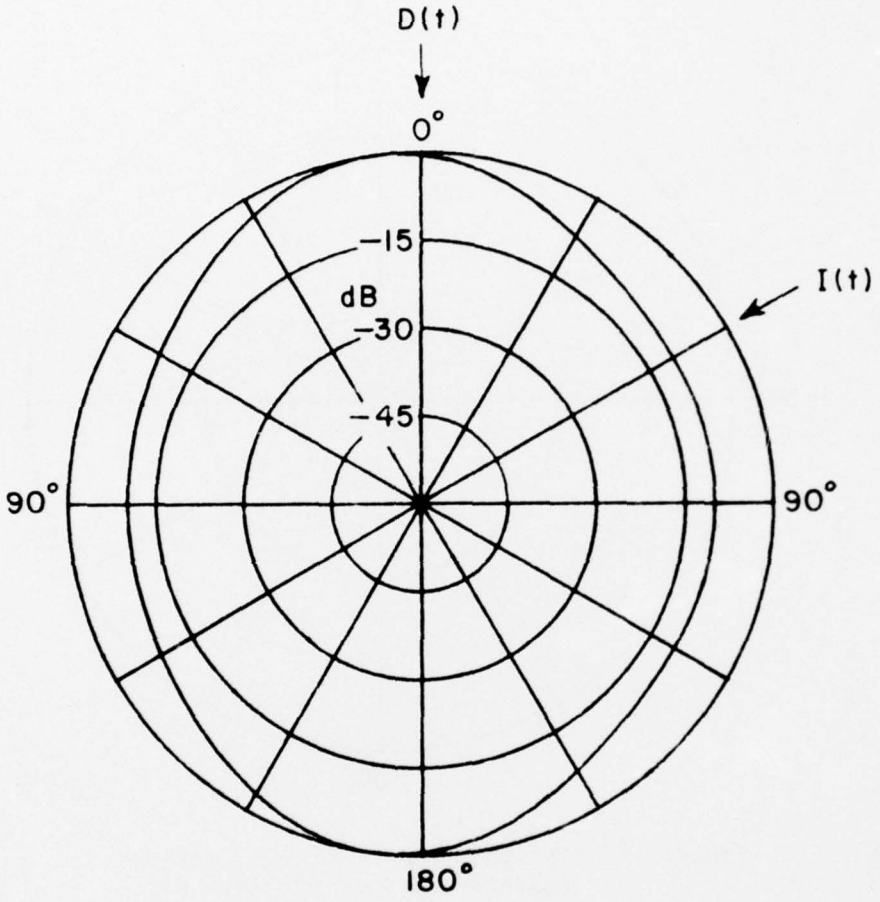

Figure 13. Pattern after 1 time constant.

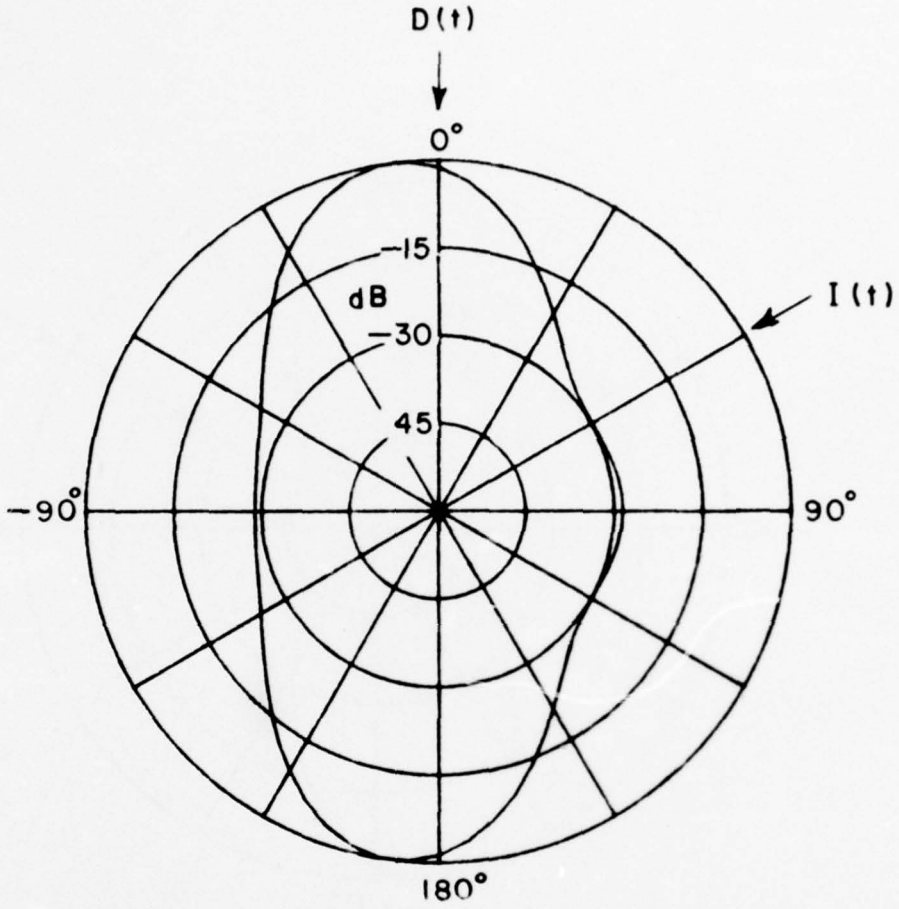

Figure 14. Pattern after 2 time constant.
Pattern computed at f=455 KHz.

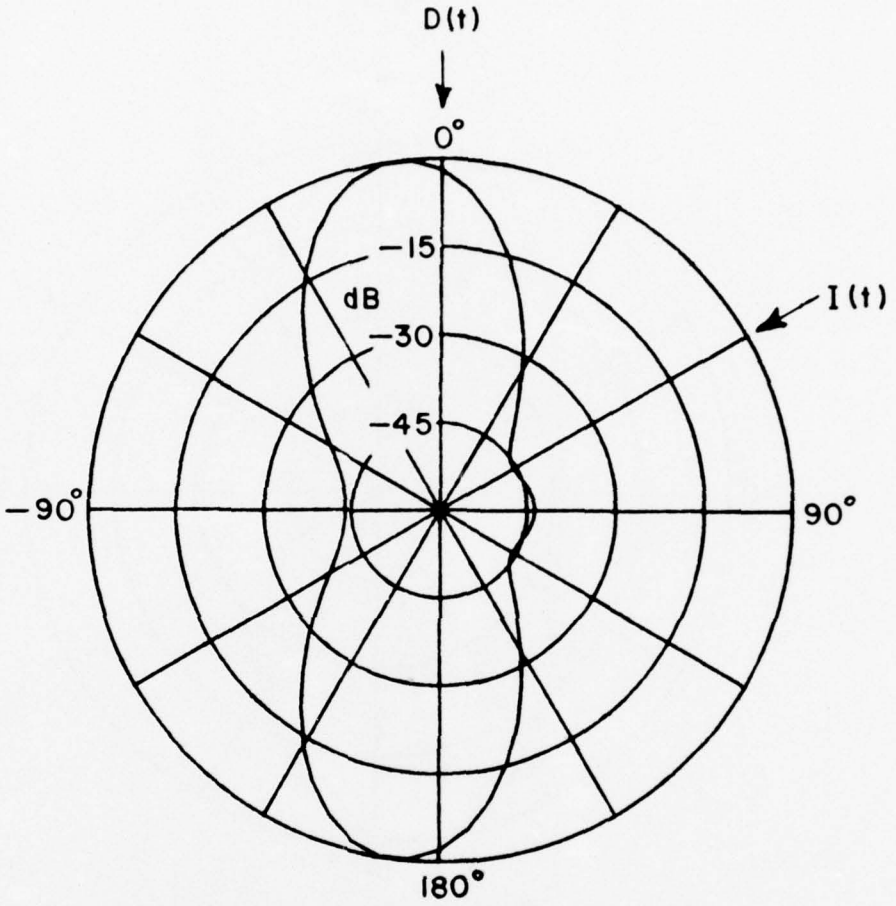

Figure 15. Pattern after 3 time constant.
Pattern computed at f=455 KHz.

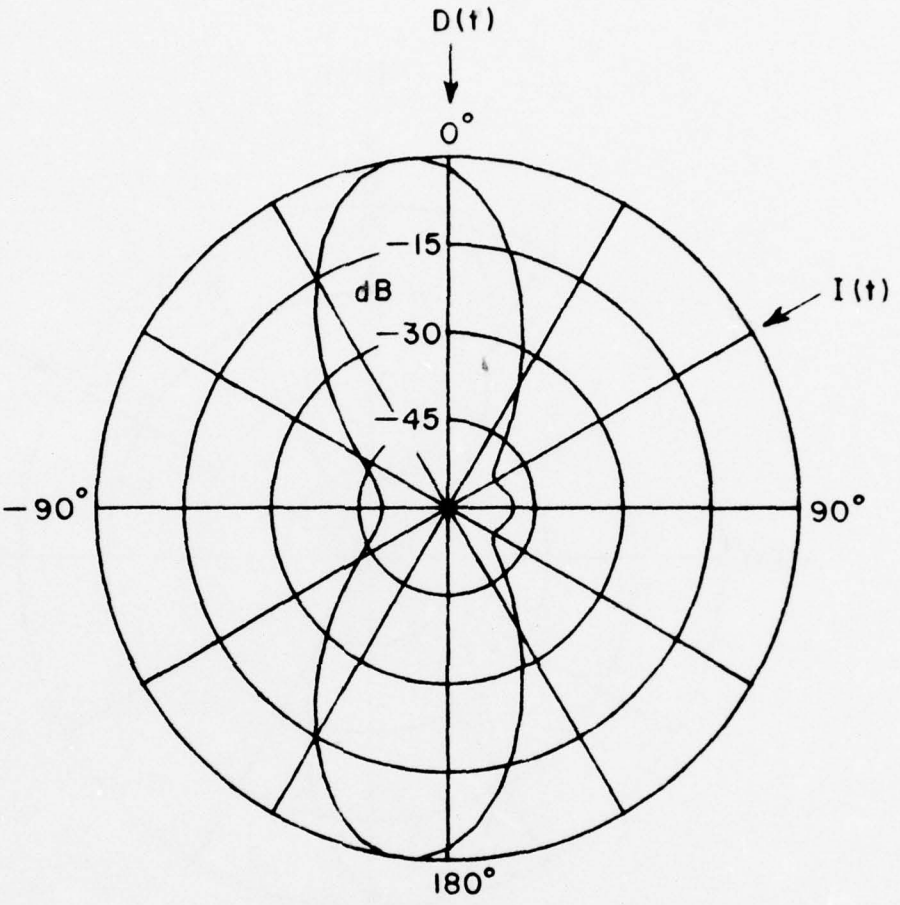

Figure 16. Pattern after 4 time constant.
Pattern computed at f=455 KHz.

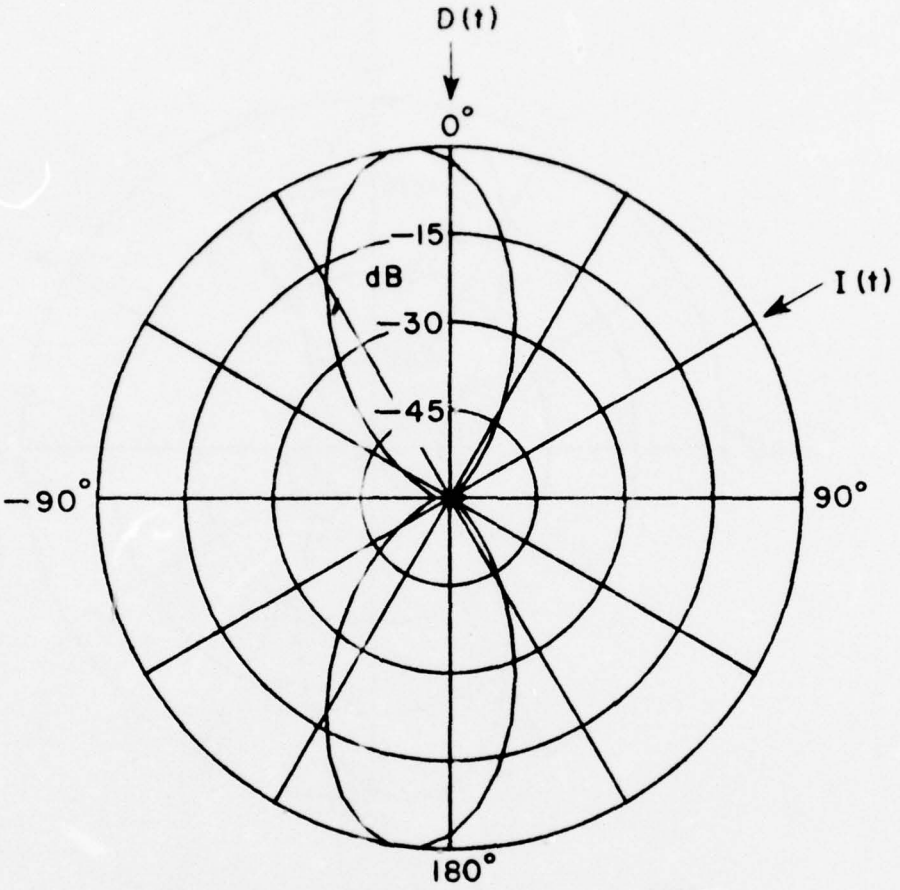

Figure 17. Final pattern. Pattern computed at f=455 KHz.

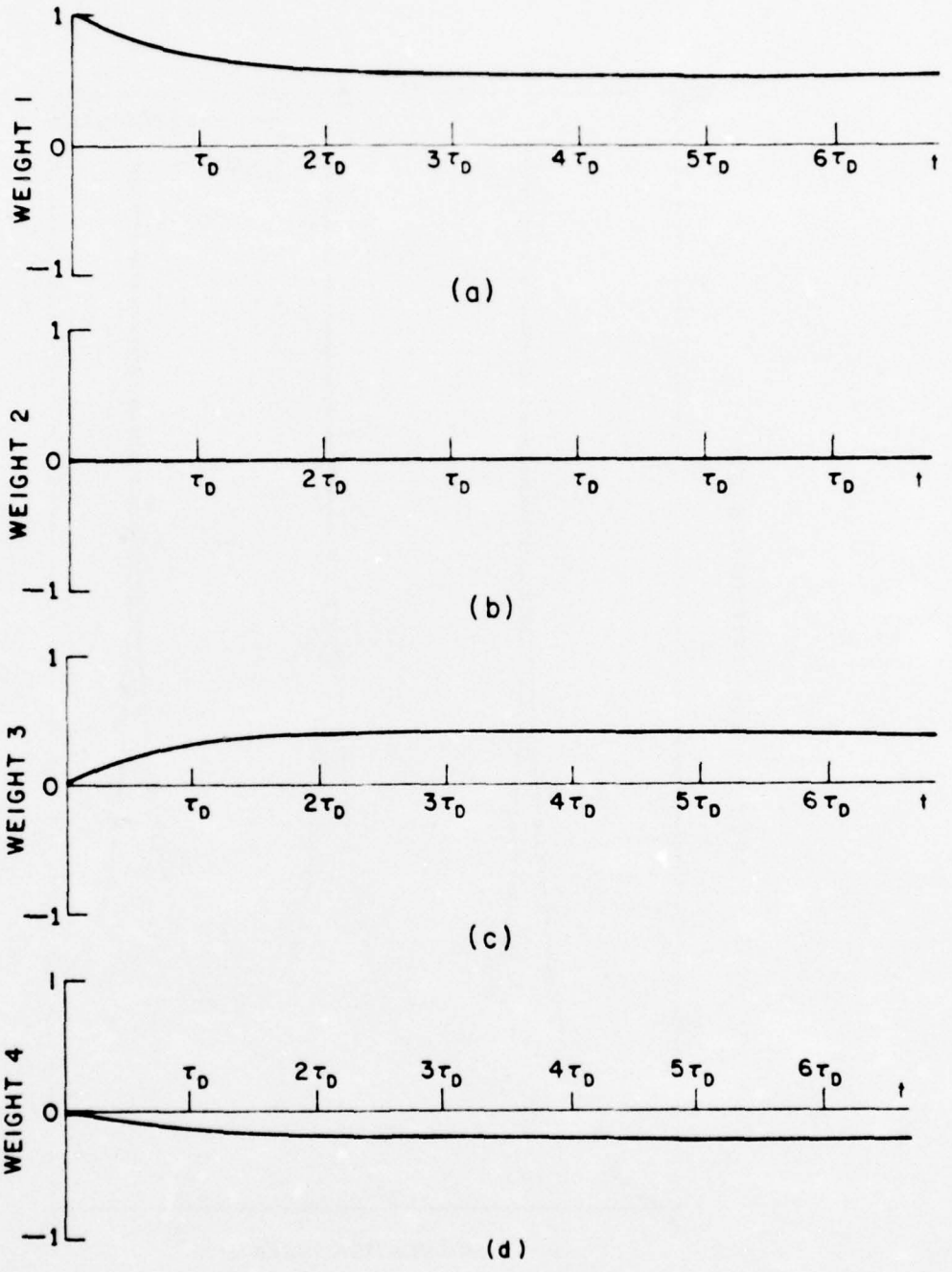

Figure 18. Transient behavior of the weights (a) weight 1, (b) weight 2, (c) weight 3 and (d) weight 4.

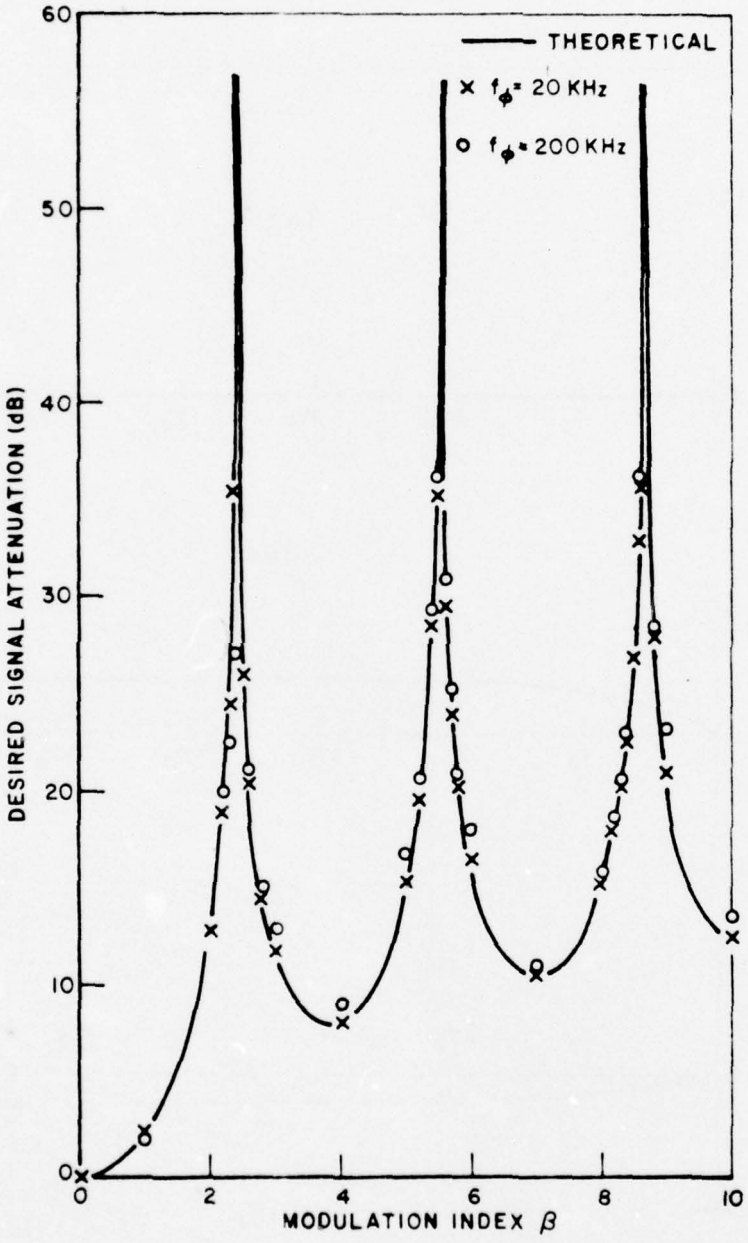

Figure 19a. Effect of the modulation index on the output desired signal attenuation.

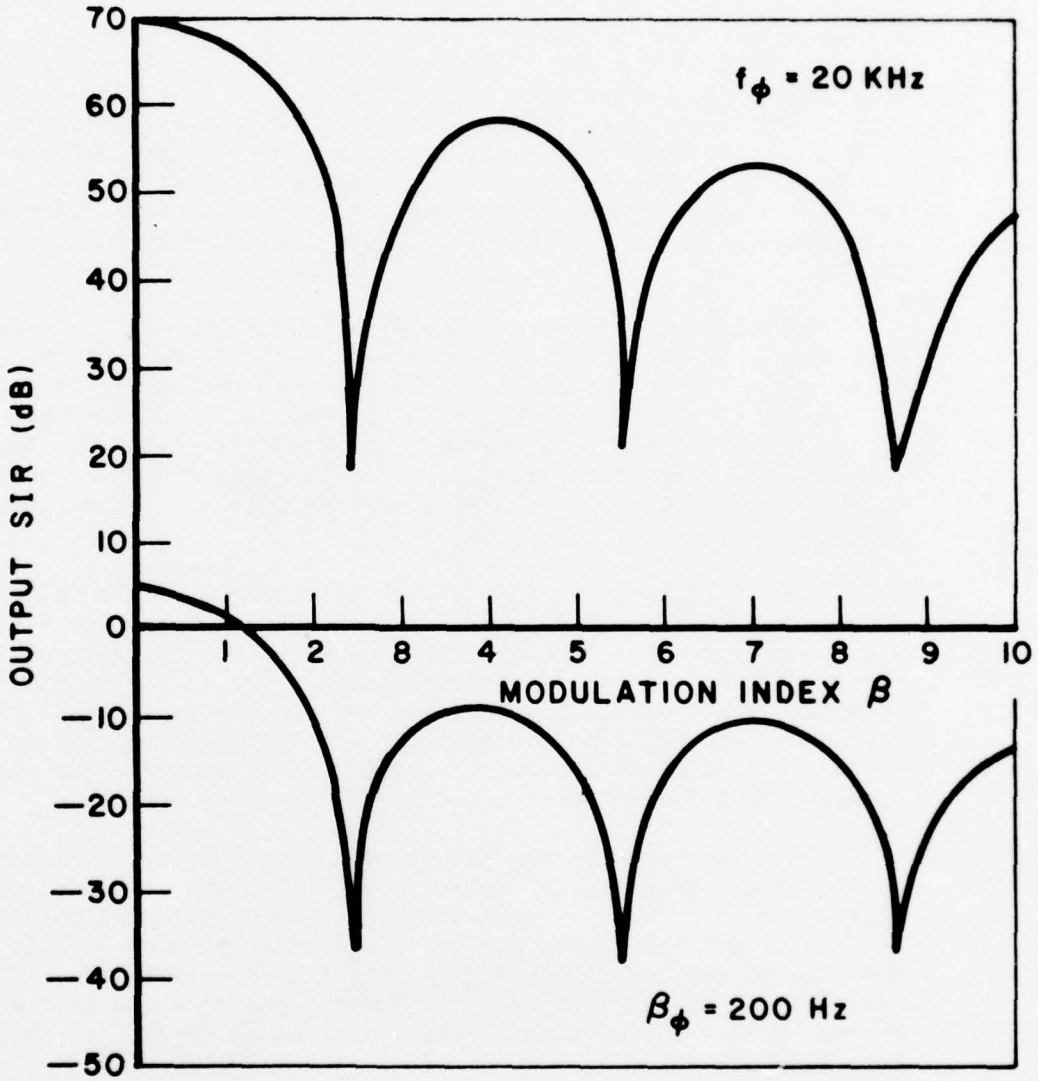

Figure 19b. Effect of the modulation index on the output signal-to-interference ratio.

In general, as the modulation index increases, the desired signal bandwidth increases and the reference signal without FM becomes a poorer estimate of D(t), so there is less correlation between them, and the output ADS increases.

Figure 19b shows the corresponding output SIR derived from the computer simulation of the LMS algorithm. (The output SIR as obtained from a theoretical calculaton based on Equations (64) to (66) is not meaningful, because the infinite time average completely decorrelates the interference and reference signal. As a result there is no output interference power in that model.) If we compare these 2 output SIR curves with the corresponding ADS curves in Figure 19a, it appears that the output interference power is constant for all β. We would expect this result, since the correlation between I(t) and R(t) is independent of β. The output SIR decreases when the output desired power decreases, because β affects the output desired power.

Moreover, for a fixed β the array suppresses the interference much more when f_ϕ = 20 KHz than f_ϕ = 200 Hz. This result occurs because the higher f_ϕ, the more the spectral components of the product R(t)I(t) are spread beyond the bandwidth of the feedback loop. For f_ϕ = 200 Hz, the first harmonic of R(t)I(t) at 200 Hz lies within the feedback loop bandwidth. As a result, this harmonic contributes to the weight jitter and causes the array not to null the interference as well.

From the above results, if the attenuation of the desired signal must be held within 10 dB, the value for β must be chosen less than 1.8. Therefore this type of reference signal is suitable only for narrowband FM. It is also seen that the array will null the interference signal effectively provided the correlation product of I(t) R(t) does not have significant power within the feedback loop bandwidth, that is, when the code frequency f_ϕ is high enough. (Recall however, that f_ϕ must not exceed f_{min}! (See Equation (45)).)

Next, we consider the effect of the square wave timing offset on the array performance. We assume no frequency offset on the desired carrier. Figures 20a and 20b show the attenuation of the desired signal and the output signal-to-interference ratio as a function of the percentage square wave timing offset with β as a parameter. The conditions of the input signal are the same as those in Figure 19. The switching rate is set equal to 20 KHz. In Figure 20a, for a fixed β the ADS increases as the timing offset increases. If a maximal length PN code is used in this simulation instead of

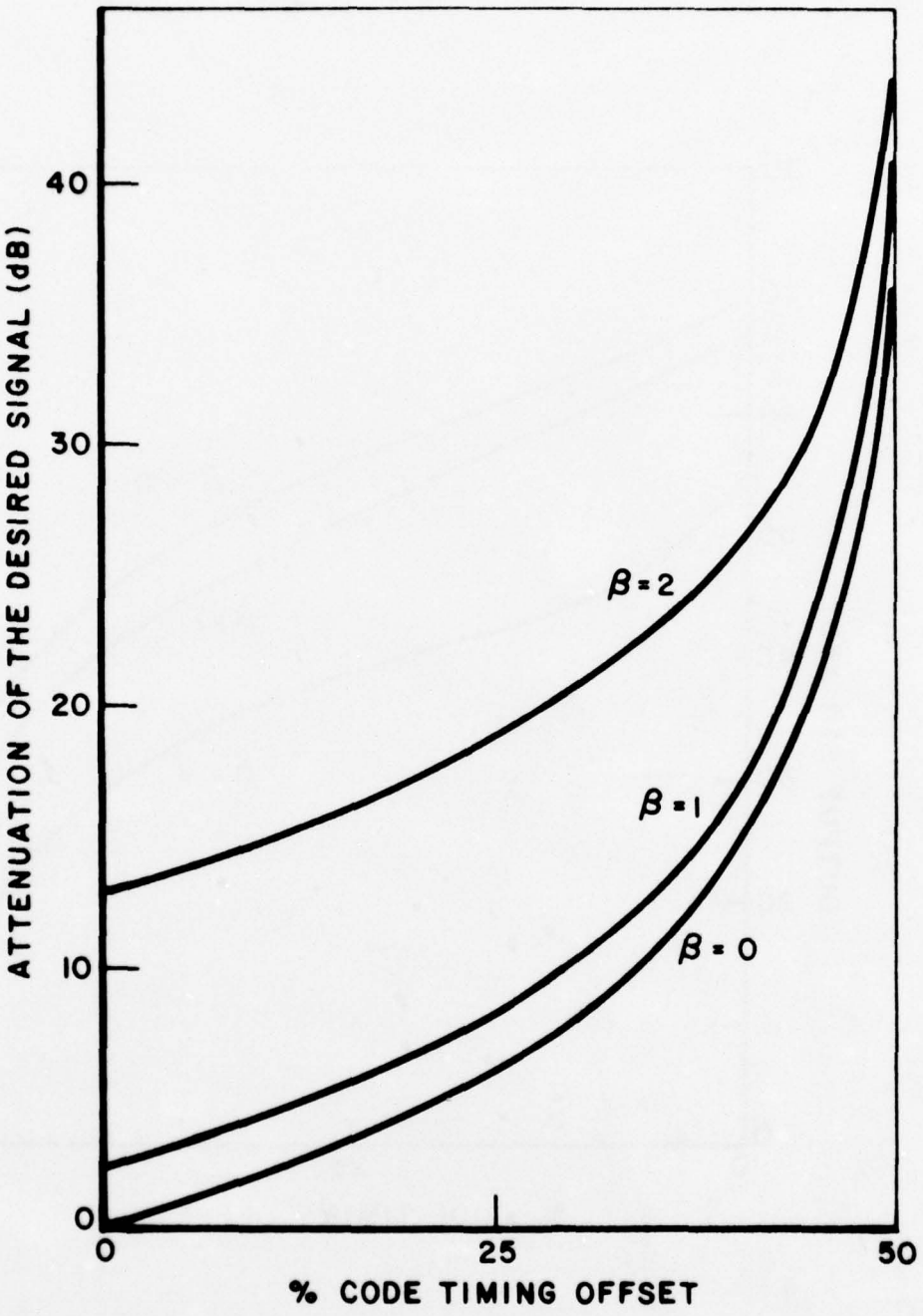

Figure 20a. Effect of the code timing offset on the output desired signal attenuation.

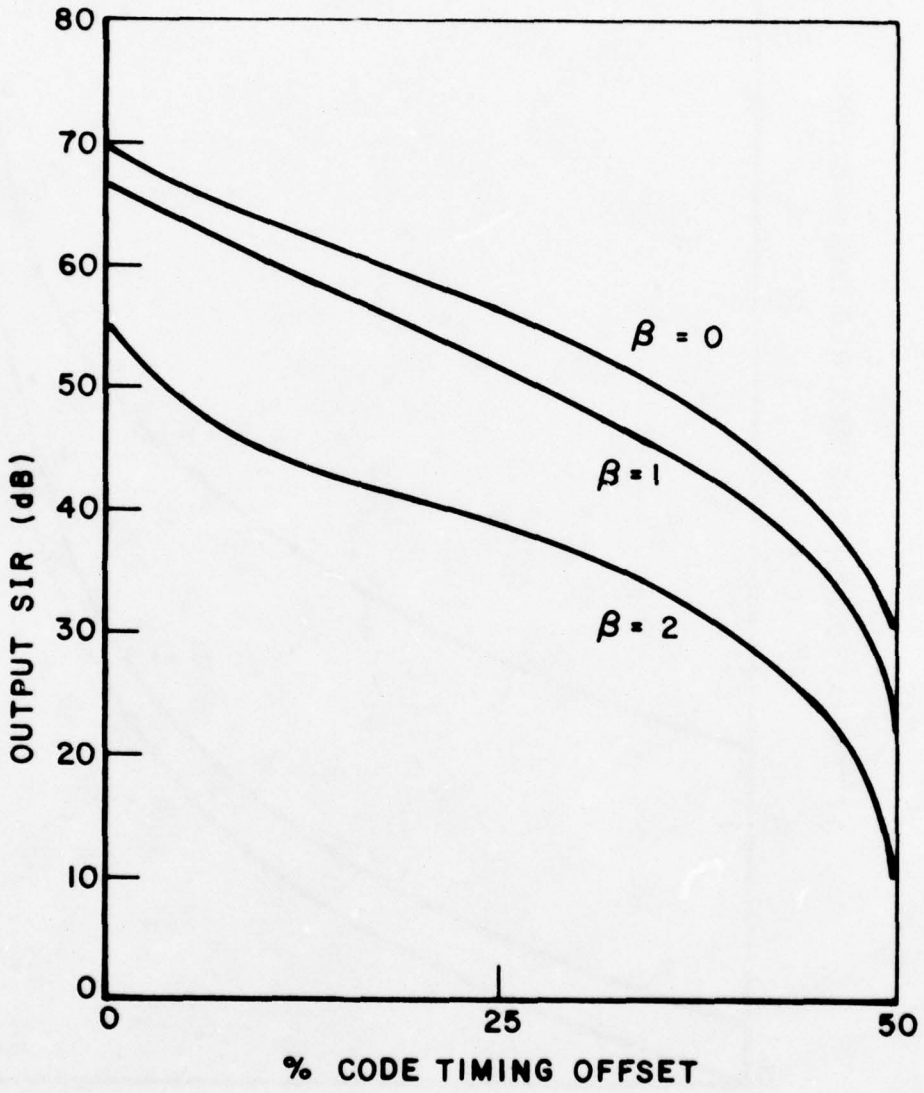

Figure 20b. Effect of the code timing offset on the output signal-to-interference ratio.

the square wave, the desired signal attenuation is approximately 7 dB* (for β=0) at 50% code timing offset rather than 36 dB (β=0) as shown for the square wave. To understand this statement, consider the simple case where β=0. If there is no FM modulation on the desired signal, both the desired and the reference signals are bi-phase modulated sine waves. The cross correlation between these two signals is equal to the autocorrelation function of the PN code or the square wave, both of which are shown in Figure 21. We see that the correlation becomes zero at a 1/2 bit offset for the square wave, while it does not become zero until a one bit offset for the PN code. Due to the symmetry property of the square wave, the ADS from 50% to 100% square wave timing offset is just the mirror image of that from 0% to 50%. This portion of the curves is not shown in Figure 20a. Of course, if a maximal length PN code is used, the symmetry property no longer exists. For a fixed square wave timing offset, the ADS increases as β becomes large. This effect is to be expected, since the reference signal is a simple bi-phase modulated sine wave, which becomes a poorer estimate of the FM desired signal as β increases.

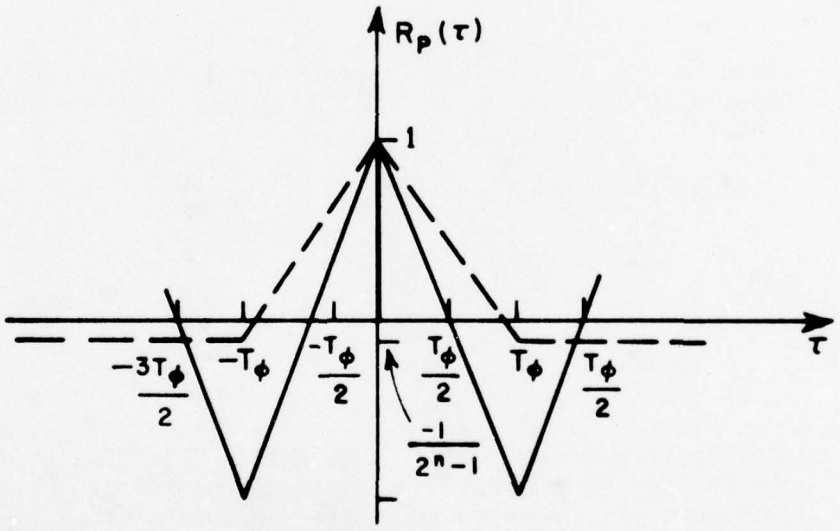

21. The autocorrelation function of a square wave (___) and of a maximal length PN code (---). (T_ϕ is the bit interval.) n is the number of stages in the shift register used to generate the code.

* If β=0 and a maximal length PN code is used, this case is identical to that in Figure 11.

In Figure 20b, we see that the output SIR drops as the square wave timing offset increases. The decrease of the SIR is primarily due to the desired signal being attenuated. Since the phase modulation is not present on the interference signal, the correlation between the interference and reference signal is not affected by the square wave timing offset. Furthermore, with f_ϕ set at 20 KHz, the output interference power is negligibly small.

From the above results, we see that for a maximal length PN code sequence, the code timing difference between the desired and reference signals should not exceed half a bit.

Finally the effect of the desired signal carrier frequency offset on the performance of the array is studied in Figures 23a and 23b with β as parameter. We assume the desired carrier deviates from $\omega_c(2\pi(455 \times 10^3)$ rad/sec) (to simulate transmitter frequency inaccuracies or Doppler shift). Thus the desired signal is given by

$$D(t) = A \sin [(\omega_c + \Delta\omega)t + \beta \sin \omega_m t + \phi(t)] \quad , \tag{82}$$

where $\Delta\omega = |\omega_d - \omega_c|$. The reference and interference signals are assumed to be the same as those in Figures 19a and 19b, i.e.,

$$R(t) = A \sin [\omega_c t + \phi(t)] \tag{83}$$

and

$$I(t) = B \sin \omega_c t \tag{84}$$

$\phi(t)$ is a square wave at f_ϕ = 20 KHz in this simulation. For $\beta \leq 2$, the Fourier transform of the correlation product $D(t)R(t)$ is shown in Figure 22. The frequency offset has eliminated the dc term of $D(t)R(t)$ as seen in Figure 22. This dc term determines the correlation between the desired and reference signals. As $\Delta\omega$ increases, the desired-reference product has less power within the feedback loop bandwidth ($2\pi(1.45 \times 10^3)$ rad/sec in this case). Figure 23a shows the desired signal attenuation as a function of the frequency offset. We see that for a fixed β the desired signal attenuation increases as the frequency offset increases. When $\Delta\omega$ is greater than the feedback loop bandwidth, the significant component of $R(t)$ $D(t)$ at $\Delta\omega$ is filtered out by the feedback loop. Thus the desired signal suffers a heavy attenuation. For a given percentage frequency offset, the ADS increases when β increases. Again, this effect is

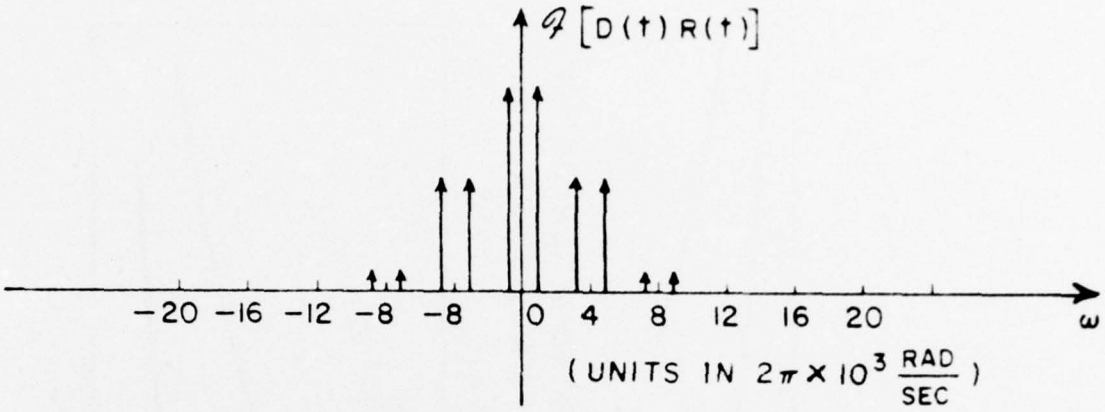

Figure 22. The correlation product of the desired and reference signal. ($\Delta\omega$ varying).

expected because increasing β decreases the correlation between the desired and reference signals.

Figure 23b shows the output signal-to-interference ratio versus the frequency offset. It is seen that for a fixed β, the output SIR decreases as the frequency offset increases. If we compare the two SIR curves with the 2 ADS curves in Figure 23a, it is seen that the output interference power is constant for all frequency offsets. This behavior is what we would expect, because the frequency offset on the desired carrier does not affect the correlation between the interference and reference signals.

From the above results, we conclude that to maintain high correlation between the reference and desired signals, the desired signal carrier offset must not be larger than the feedback loop bandwidth. The feedback loop bandwidth, in turn, is constrained to be less than the minimum audio modulation frequency (see Equation (47)). As a result, this type of system is rather sensitive to frequency offset.

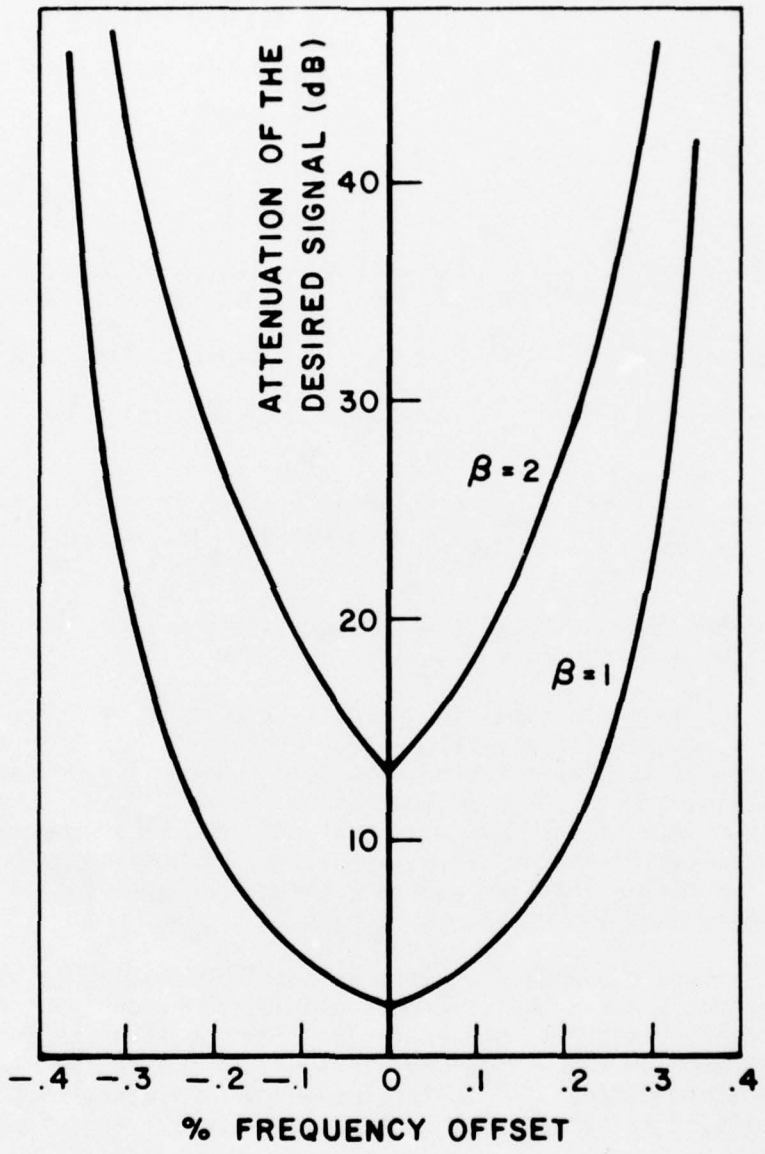

Figure 23a. Effect of the frequency offset on the output desired signal attenuation.

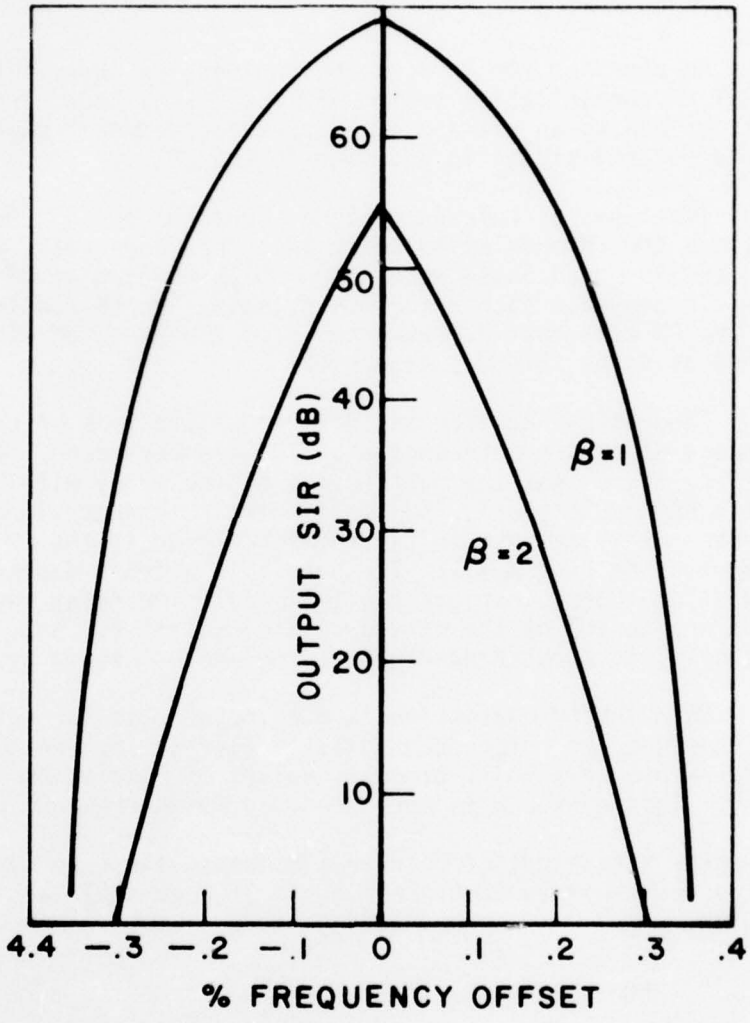

Figure 23b. Effect of the frequency offset on the output signal-to-interference ratio.

CHAPTER IV

CONCLUSIONS

An approach for integrating an adaptive array into a conventional FM communication system has been suggested. The method consists of adding an extra digital pseudonoise coded phase modulation to the desired signal in addition to the FM.

Two types of reference signals were proposed. One of them includes the FM modulation while the other does not. Both types contain the PN coded phase modulation which appears on the desired signal. To generate such reference signals, the FM modulating signal and the PN code must be extracted from the received signal. A method of doing this was suggested.

Theoretical studies and digital simulations of the array performance with such reference signals have been done. The results indicate first that the performance of the array will be much better if the FM modulation is included in the reference signal. However, when the FM is present on the reference signal, the FM modulation delay must be kept small. The permissible delay depends upon the modulation index. For example the modulation delay cannot exceed about one tenth* of the minimum audio cycle** for $\beta=3$. The permissible delay is about a quarter* of the minimum audio cycle for $\beta=1$.

When the FM modulation is not included in the reference signal (which makes the reference signal simpler to implement), the array operates properly only for small values of modulation index ($\beta << 1.8$*). This approach is suitable only for narrowband FM.

For both kinds of reference signals, the code timing offset must be kept within about half a bit if a maximal length PN code is used.

---

* These values are based on the assumption that a system can tolerate 10 dB attenuation on the desired signal.

** See the footnote on Page 57.

Finally, the array performance for either type of reference signal is very sensitive to the desired signal frequency offset. The frequency offset on the desired signal carrier should be less than the feedback loop bandwidth, which in turn has to be less than the minimum modulation frequency. For β=1, the maximum frequency offset is approximately 60%* of the feedback loop bandwidth. These results mean that the frequency must be accurately controlled (or tracked) in such a system.

* We assume a system can tolerate 10 dB desired signal attenuation.

REFERENCES

1. Widrow, B., Mantey, P.E., Griffiths, L.J., and Godde, B.B., "Adaptive Antenna Systems," Proc. IEEE, 55, 12 (December 1967), pp. 2143-2159.

2. Riegler, R.L. and Compton, R.T., Jr., "An Adaptive Array for Interference Rejection," Proc. IEEE, 61, 6 (June 1973), p. 748.

3. Applebaum, S.P., "Adaptive Arrays," Special Projects Laboratory Report SPL-TR66-1, August 1966, Syracuse University Research Corporation, Syracuse, N.Y.

4. Stiffler, J.J., Theory of Syncrhonous Communications, Prentice-Hall, Inc., Englewood Cliffs, New Jersey, (1971), p. 178.

5. Birdsall, T.G. and Ristenbatt, M.P., "Introduction to Linear Shift-Register Generated Sequences," The University of Michigan Research Institute, Report 90 (October 1958).

6. Ziemer, R.E. and Tranter, W.H., Principles of Communication, System, Modulation and Noise, Houghton Mifflin Co., Boston (1976), p. 134.

7. Gill, W.J., "A Comparison of Binary Delay-Lock Tracking-Loop Implementations," IEEE Trans., AES-2, 4 (July 1966), p. 415.

8. Spilker, J.J., Jr. and Magil, D.T., "The Delay-Lock Discrimination---An Optimum Tracking Device," Proc. IER, 49, 9 (September 1961), p. 1403.

9. Spilker, J.J., Jr., "Delay-Lock Tracking of Binary Signal," IEEE Trans., SET-9 (March 1963), p. 1.

10. Chan, L.C. and Compton, R.T., Jr., "An Adaptive Array Technique For AM Signals," Report 4326-3, January 1977, The Ohio State University ElectroScience Laboratory, Department of Electrical Engineering; prepared under Contract N00019-76-C-0195 for Department of the Navy.

11. Brennan, L.E., Pugh, E.L. and Reed, I.S., "Control Loop Noise in Adaptive Array Antennas," IEEE Trans., AES-7, 2 (March 1971), p. 254.

12. Koleszar, G.E., "The Stochastic Properties of the Weights in an Adaptive Antenna Array," Report 4063-1, August 1975, The Ohio State University ElectroScience Laboratory, Department of Electrical Engineering; prepared under Contract N00019-75-C-0179 for Naval Air Systems Command.

13. Miller, T.W., "The Transient Response of Adaptive Arrays in TDMA Systems," Report 4116-1, June 1976, The Ohio State University ElectroScience Laboratory, Department of Electrical Engineering; prepared under Contract F30602-75-C-0061 for Rome Air Development Center.

APPENDIX A

In this appendix, we calculate the steady state weights for the case where the reference signal is

$$R(t) = A \sin [\omega_c t + \beta \sin \omega_m (t-t_o) + \phi(t)] \quad . \tag{67}$$

The in phase and the quadrature array signals are given by Equations (59) to (62),*

$$x_1(t) = A \sin [\omega_c t + \beta \sin \omega_m t + \phi(t)] + B \sin \omega_c t \tag{59}$$

$$x_2(t) = A \cos [\omega_c t + \beta \sin \omega_m t + \phi(t)] + B \cos \omega_c t \tag{60}$$

$$x_3(t) = A \sin [\omega_c t + \beta \sin \omega_m t + \phi(t) - \gamma_d] + B \sin(\omega_c t - \gamma_i) \tag{61}$$

and

$$x_4(t) = A \cos [\omega_c t + \beta \sin \omega_m t + \phi(t) - \gamma_d] + B \cos(\omega_c t - \gamma_i) \quad . \tag{62}$$

The steady state weight vector is found from

$$W_{ss} = \begin{pmatrix} W_{ss1} \\ W_{ss2} \\ W_{ss3} \\ W_{ss4} \end{pmatrix} = \phi^{-1} S$$

---

* Here we assume there is no frequency offset on the desired signal carrier; ω_d is thus equal to ω_c.

with Φ and S defined in Equations (65) and (66) respectively.

For the signals given above we have

$$\Phi = \begin{pmatrix} \frac{A^2}{2}+\frac{B^2}{2} & 0 & \frac{A^2}{2}\cos\gamma_d+\frac{B^2}{2}\cos\gamma_i & \frac{-A^2}{2}\sin\gamma_d-\frac{B^2}{2}\sin\gamma_i \\ 0 & \frac{A^2}{2}+\frac{B^2}{2} & \frac{A^2}{2}\sin\gamma_d+\frac{B^2}{2}\sin\gamma_i & \frac{A^2}{2}\cos\gamma_d+\frac{B^2}{2}\cos\gamma_i \\ \frac{A^2}{2}\cos\gamma_d+\frac{B^2}{2}\cos\gamma_i & \frac{A^2}{2}\sin\gamma_d+\frac{B^2}{2}\sin\gamma_i & \frac{A^2}{2}+\frac{B^2}{2} & 0 \\ -\frac{A^2}{2}\sin\gamma_d-\frac{B^2}{2}\sin\gamma_i & \frac{A^2}{2}\cos\gamma_d+\frac{B^2}{2}\cos\gamma_i & 0 & \frac{A^2}{2}+\frac{B^2}{2} \end{pmatrix} \tag{85}$$

and the elements of the S matrix can be calculated as follows

$$\begin{aligned} \overline{x_1(t)R(t)} = {} & \overline{AB \sin\omega_c t \sin[\omega_c t + \beta \sin\omega_m(t-t_o) + \phi(t)]} \\ & + \overline{A^2 \sin[\omega_c t + \beta \sin\omega_m t + \phi(t)]} \\ & \overline{\sin[\omega_c t + \beta \sin\omega_m(t-t_o) + \phi(t)]} \quad . \end{aligned} \tag{86}$$

Since the PN code is included in the reference signal but not in the interference, the infinite time average eliminates the first term in Equation (86).* Thus

$$\begin{aligned} \overline{x_1(t)R(t)} &= \frac{A^2}{2} \lim_{T_W\to\infty} \frac{1}{T_W} \int_{-T_W/2}^{T_W/2} \cos[\beta(1-\cos\omega_m t_o)\sin\omega_m t \\ &\qquad + \beta \sin\omega_m t_o \cos\omega_m t]dt \qquad (87) \\ &= \frac{A^2}{2} \lim_{T_W\to\infty} \frac{1}{T_W} \int_{-T_W/2}^{T_W/2} \cos[\rho\beta\cos(\omega_m t - \gamma)]\, dt \end{aligned}$$

---

* We assume that $\omega_\phi \neq \omega_m$. If $\omega_\phi = \omega_m$, a spectral line of I(t)R(t) will fall at dc and the above analysis will not apply. The real modulation signal we envision is an audio signal with power distributed continuously between ω_{min} and ω_{max}. We then choose ω_ϕ to be less than ω_{min} to prevent a dc term in I(t)R(t).

where

$$\rho = \sqrt{(1 - \cos \omega_m t_o)^2 + \sin^2 \omega_m t_o} = 2 \sin\left(\frac{\omega_m t_o}{2}\right) \quad , \tag{88}$$

$$\gamma = \tan^{-1}\left(\frac{1-\cos\omega_m t_o}{\sin\omega_m t_o}\right) \quad , \tag{89}$$

and T_W is a time window over which the integration is performed. Since the integrand is periodic, the infinite time average may be replaced by an average over one period of the integrand

$$\overline{x_1(t)R(t)} = \frac{A^2}{2} \frac{\omega_m}{2\pi} \int_{-\pi/\omega_m}^{\pi/\omega_m} \cos[\rho\beta \cos(\omega_m t - \gamma)]dt \quad . \tag{90}$$

If we let $x=\omega_m t$, Equation (90) becomes

$$x(t)R(t) = \frac{A^2}{2} \frac{\omega_m}{2\pi} \int_{-\pi}^{\pi} \cos[\rho\beta \cos(\omega_m t - \gamma)]dt$$

$$= \frac{A^2}{2} J_o(\rho\beta) \tag{91}$$

where $J_o(\ )$ is the zero order Bessel function. Finally

$$\overline{x_1(t)R(t)} = \frac{A^2}{2} J_o\left[2\beta \sin\left(\frac{\omega_m t_o}{2}\right)\right] \quad . \tag{92}$$

Similarly we find

$$\overline{x_2(t)R(t)} = 0 \tag{93}$$

$$\overline{x_3(t)R(t)} = \frac{A^2}{2} (\cos \gamma_d) J_o\left[2\beta \sin\left(\frac{\omega_m t_o}{2}\right)\right] \tag{94}$$

and

$$\overline{x_4(t)R(t)} = \frac{A^2}{2} (\sin \gamma_d) J_o\left[2\beta \sin\left(\frac{\omega_m t_o}{2}\right)\right] \quad . \tag{95}$$

The elements of the S matrix all contain the zero order Bessel functions of argument $2\beta\sin(\omega_m t_o)/2)$,

$$S = \begin{pmatrix} \frac{A^2}{2} \\ 0 \\ \frac{A^2}{2}\cos\gamma_d \\ \frac{A^2}{2}\sin\gamma_d \end{pmatrix} J_o\left[2\beta \sin\left(\frac{\omega_m t_o}{2}\right)\right] \quad . \tag{96}$$

The steady state weights can be obtained by substituting the inverse of Φ in Equation (85) and Equation (96) into Equation (64).

If we let θ_d=0°, θ_i=60°, A=1 and B=10, the inverse of Φ can easily be computed. The result is

$$\Phi^{-1} = \begin{pmatrix} .52804 & 0. & .47195 & .21361 \\ 0. & .52804 & -.21361 & .47195 \\ .47195 & -.21361 & .52804 & 0. \\ .21361 & .47195 & 0. & .52804 \end{pmatrix} \quad . \tag{97}$$

The steady state weight vector corresponding to this special case is

$$W_{ss} = \begin{pmatrix} .5 \\ -.1068 \\ .5 \\ .1068 \end{pmatrix} J_o\left[2\beta \sin\left(\frac{\omega_m t_o}{2}\right)\right] \quad . \tag{98}$$

APPENDIX B

In this appendix we assume the PN codes in the reference and desired signals are not synchronized. Thus the reference signal has the form

$$R(t) = A \sin[\omega_c t + \beta \sin \omega_m t + \phi(t-\tau)] \quad . \tag{69}$$

The in phase and quadrature array signals are defined in Appendix A.

To calculate the steady state weights, we must know the matrices Φ and S. Since the input signals are the same as those in Appendix A, the Φ matrix does not change (see Equation (85)). The elements of the S matrix can be calculated as follows:

$$\overline{x_1(t)R(t)} = \frac{A^2}{2} \left\{ \overline{\cos[\phi(t) - \phi(t-\tau)]} - \overline{\cos[2\omega_c t + 2\beta \sin \omega_m t + \phi(t) + \phi(t-\tau)]} \right\} . \tag{99}$$

The infinite time average eliminates the second term and hence Equation (99) becomes

$$\overline{x_1(t)R(t)} = \frac{A^2}{2} \overline{P(t)P(t-\tau)} \tag{100}$$

where P(t) is a periodic PN code of period T_p as shown in Figure 2b. The limiting process in Equation (100) is then not necessary and $\overline{x_1(t)R(t)}$ can be simplified to give

$$\overline{x_1(t)R(t)} = \frac{A^2}{2} \frac{\int_0^{T_p} P(t)P(t-\tau)dt}{T_p} = \frac{A^2}{2} R_p(\tau) \tag{101}$$

where $R_p(\tau)$ is the autocorrelation function of P(t) [5] and is shown in Figure 21. If the number of stages in the shift register generating the PN code is large, $R_p(\tau)$ may be approximated by Equation (72). We also find

$$\overline{x_2(t)R(t)} = 0 \tag{102}$$

$$\overline{x_3(t)R(t)} = \frac{A^2}{2} R_p(\tau)\cos \gamma_d \tag{103}$$

and

$$\overline{x_4(t)R(t)} = \frac{A^2}{2} R_p(\tau)\sin \gamma_d \quad . \tag{104}$$

With $\theta_d=0°$, $\theta_i=60°$, A=1 and B=10, the steady state weight vector can be computer as follows:

$$W_{ss} = \Phi^{-1}S = \begin{pmatrix} .52804 & 0. & .47195 & .21361 \\ 0. & .52804 & -.21361 & .47195 \\ .47195 & -.21361 & .52804 & 0. \\ .21361 & .47195 & 0. & .52804 \end{pmatrix} \begin{pmatrix} .5 \\ 0 \\ .5 \\ 0 \end{pmatrix} R_p(\tau)$$

$$= \begin{pmatrix} .5 \\ -.1068 \\ .5 \\ .1068 \end{pmatrix} R_p(\tau) \quad . \tag{105}$$

APPENDIX C

```
C***  THE TWO-ELEMENT LMS ARRAY WITH THE METHOD OF STEEPEST DESCENT
C***  ********************************************************
      $OPTIONS 32K
      $OPTIONS DP
      INCLUDE POLPLS
      DIMENSION *E4(2500),*E3(2500),*E2(2500),*E1(2500),*(4),X(4)
     $,PAI(361),OUTSI(2500)
      COMMON *E1,*E2,*E3,*E4
      DATA PI,TPI,HPI/3.14159265359,6.28318530718,1.57079632679/
1200  FC=455.E 03
      FM=4220\
      FJ=450.E 03
      WRITE(8,31)
31    FORMAT('BETA=')
      READ(8,22) BETA
      DE=.0025
      ANGLE=0.
      ANGLJ=90.
      WRITE(8,21)
21    FORMAT('GAM(DEGREE)=')
      READ(8,22) GAM
22    FORMAT(F20.5)
      FS=10.*FC
      TS=1./FS
      WM=TPI*FM
      WC=TPI*FC
      WJ=TPI*FJ
      EDE=PI*SIN(ANGLE*PI/180.)
      EDJ=(FJ*PI*SIN(ANGLJ*PI/180.))/FC
      *(1)=1.0
      *(2)=0.0
      *(3)=0.0
      *(4)=0.0
      T=0.
25    DO 1 JI=1,2500
C***  THE INPUT SIGNAL
C***  ****************
      OMETJ=WJ*T
      IF(OMETJ.GT.TPI) GO TO 51
      GO TO 52
51    OMETJ=OMETJ-TPI
      IF(OMETJ.GT.TPI) GO TO 51
C
52    OMETMI=WM*T
      IF(OMETMI.GT.TPI) GO TO 11
      GO TO 12
11    OMETMI=OMETMI-TPI
      IF(OMETMI.GT.TPI) GO TO 11
C
12    *TDI=WC*T+BETA*SIN(OMETMI)
      IF(*TDI.GT.TPI) GO TO 13
      GO TO 14
13    *TDI=*TDI-TPI
      IF(*TDI.GT.TPI) GO TO 13
      GO TO 16
14    IF(*TDI.LT.-TPI) GO TO 15
      GO TO 16
15    *TDI=*TDI+TPI
      IF(*TDI.LT.-TPI) GO TO 15
16    X(1)=SIN(*TDI)+12.*SIN(OMETJ)
      X(2)=SIN(*TDI-HPI)+12.*SIN(OMETJ-HPI)
      X(3)=SIN(*TDI+EDE)+12.*SIN(OMETJ+EDJ)
      X(4)=SIN(*TDI+EDE-HPI)+12.*SIN(OMETJ+EDJ-HPI)
C***  THE REFERENCE SIGNAL
C***  ********************
```

```
      OMETMR=WM*.-GR*PI/180.
      IF(OMETMR.GT.TPI) GO TO 41
      GO TO 42
41    OMETMR=OMETMR-TPI
      IF(OMETMR.GT.TPI) GO TO 41
C
42    WTDR=WC*T+BETA*SIN(OMETMR)
      IF(WTDR.GT.TPI) GO TO 43
      GO TO 44
43    WTDR=WTDR-TPI
      IF(WTDR.GT.TPI) GO TO 43
      GO TO 46
44    IF(WTDR.LT.-TPI) GO TO 45
      GO TO 46
45    WTDR=WTDR+TPI
      IF(WTDR.LT.-TPI) GO TO 45
46    R=SIN(WTDR)
C     THE OUTPUT SIGNAL
C     *****************
      S=0.0
      DO 3 I3=1,4
3     S=S+W(I3)*X(I3)
      OUTS1(JJ)=S
C     THE ERROR SIGNAL
C     ****************
      ERS1=R-S
C     THE NEXT W VALUE
C     ****************
      WE1(JJ)=W(1)
      WE2(JJ)=W(2)
      WE3(JJ)=W(3)
      WE4(JJ)=W(4)
      DO 2 I2=1,4
2     W(I2)=W(I2)+G*ERS1*X(I2)
1     T=T+DS
      WRITE(8,24)
24    FORMAT('CONTINUE ADAPTING=-1 CALLEXIT=0 PLOT=1,  III=')
      READ(8,-) III
      IF(III) 26,999,118
118   CALL PL(WE1)
      WRITE(8,27)
27    FORMAT('CONTINUE ADAPTING=-1, PATTERN=0')
      READ(8,-) LIK
      IF(LIK)26,119,119
119   W1=0.
      W2=0.
      W3=0.
      W4=0.
      POUT=0.
      DO 4 I4=1353,2500
      W1=WE1(I4)+W1
      W2=WE2(I4)+W2
      W3=WE3(I4)+W3
      W4=WE4(I4)+W4
4     POUT=OUTS1(I4)*OUTS1(I4)+POUT
      W1=W1/1138.
      W2=W2/1138.
      W3=W3/1138.
      W4=W4/1138.
      POUT=POUT/1138.
      WRITE(8,-)W1,W2,W3,W4,POUT
23    WRITE(8,55)
55    FORMAT('FREQ=')
      READ(8,56) FREQ
56    FORMAT(F20.6)
      DO 5 I5=1,361
```

```
      GOC=I5-1
      PHSE=(FREQ*PI*SUM(PI*GOC/180.))/FC
      W1=W1+W3*COS(PHSE)+W4*SIN(PHSE)
      W2=-W2+W3*SIN(PHSE)-W4*COS(PHSE)
5     PAT(I5)=50.*(W1*W1+W2*W2)
      DO 6 I6=1,100,5
6     WRITE(8,49) PAT(I6)
49    FORMAT(E16.4)
      PAUSE
      CALL POLPLT(PAT,2.,5)
      WRITE(8,32)
32    FORMAT('REPLOT=-1, START OVER=0, CONTINUE ADAPTING=1')
      READ(8,-)LLL
      IF(LLL) 23,1000,26
999   CALL EXIT
      END
CCC
      SUBROUTINE PL(Y)
      DIMENSION Y(1)
      CALL ASKPLT(520,3)
      CALL PLOT(4.,.7,-3)
      CALL AXIS(1.,2.,1H ,1,2.,180.,-1.,1.,1.,0)
      CALL AXIS(0.,2.,1H ,0,12.,50.,1.,250.,1.,0)
      V=-Y(1)
      H=2.
      CALL PLOT(V,H,3)
      DO 5 I3=2,2500
      V=-Y(I3)
      H=FLOAT(I3-1)/250.
5     CALL PLOT(V,H,2)
      CALL PLOT(4.5,-.7,999)
      RETURN
      END
```

APPENDIX D

In this appendix, we calculate the array steady state weight vector when the reference signal is given by

$$R(t) = A \sin[\omega_c t + \phi(t)] \tag{106}$$

and the input signals are defined by Equations (59) through (62). Note that the code timing in the desired and reference signals is assumed to be synchronized and there is no frequency offset in the desired signal ($\omega_d = \omega_c$).

The final weight vector is found from Equation (64). Since the input signals are the same as those in the Appendix A, ϕ^{-1} is the same as in Equation (97). From the above signals, the elements of the S matrix can be computed as follows:

$$\overline{x_1(t)R(t)} = A^2 \overline{\sin[\omega_c t + \beta \sin \omega_m t + \phi(t)] \sin[\omega_c t + \phi(t)]}$$

$$+ AB \overline{\sin \omega_c t \sin[\omega_c t + \phi(t)]} \quad . \tag{107}$$

The infinite time average makes the 2nd term zero due to the absence of the PN code in the interference signal. Equation (107) may be written

$$\overline{x_1(t)R(t)} = \lim_{T_W \to \infty} \frac{A^2}{T_W} \int_{-T_W/2}^{T_W/2} \cos(\beta \sin \omega_m t) dt \tag{108}$$

where T_W is the time window. Let $x = \omega_m t$, and substitute an average over one period for the limiting process. Then we have

$$\overline{x_1(t)R(t)} = \frac{A^2}{2} \frac{1}{2\pi} \int_{-\pi}^{\pi} \cos(\beta \sin x) dx = \frac{A^2}{2} J_o(\beta) \quad . \tag{109}$$

Similarly

$$\overline{x_2(t)R(t)} = 0 \quad , \tag{110}$$

$$\overline{x_3(t)R(t)} = \frac{A^2}{2} \ (\cos \gamma_d) \ J_o(\beta) \quad , \tag{111}$$

and

$$\overline{x_4(t)R(t)} = \frac{A^2}{2} \ (\sin \gamma_d) \ J_o(\beta) \quad . \tag{112}$$

Substituting Equation (97) and Equations (109) through (112) into Equation (64) yields

$$W_{ss} = \begin{pmatrix} .52804 + .47195 \cos \gamma_d \\ -.21361 \\ .47195 + .52804 \cos \gamma_d \\ .21361 \end{pmatrix} \cdot \frac{A^2}{2} \cdot J_o(\beta) \quad . \tag{113}$$

With A=1 and γ_d=0, Equation (113) becomes

$$W_{ss} = \begin{pmatrix} .5 \\ -.1068 \\ .5 \\ .1068 \end{pmatrix} J_o(\beta) \quad . \tag{114}$$